

Recent Results on Acoustic Metamaterials and Sonic Crystals

José Sánchez-Dehesa

***Wave Phenomena Group , Universitat Politècnica de València,
Camino de vera s.n., ES-46022 Valencia, Spain***

Outline

1. Introduction
2. Acoustic metamaterials with negative parameters
3. Visco-thermal effects in acoustic metamaterials with double-negative parameters
4. Sound absorption and redirection with sonic crystals based on metamaterials units



METAgenierie2017, 2-7 July.

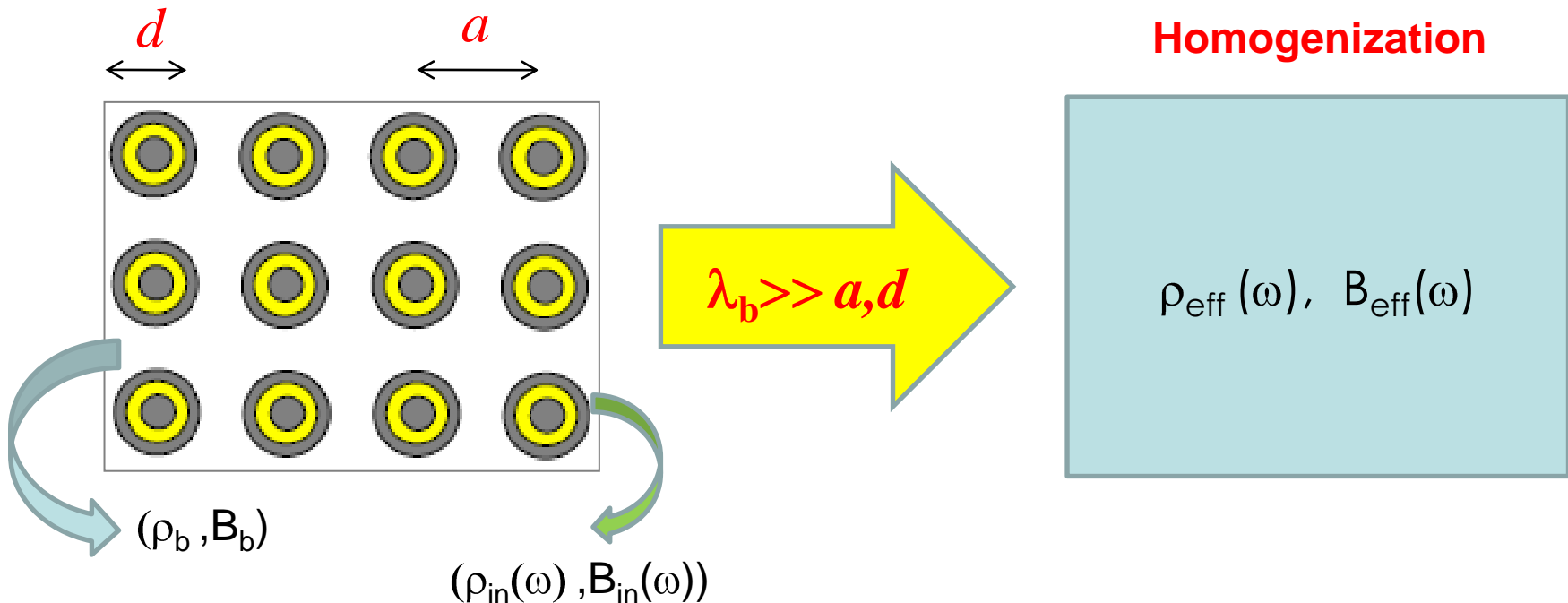
Recent Results on Acoustic metamaterials

OUTLINE

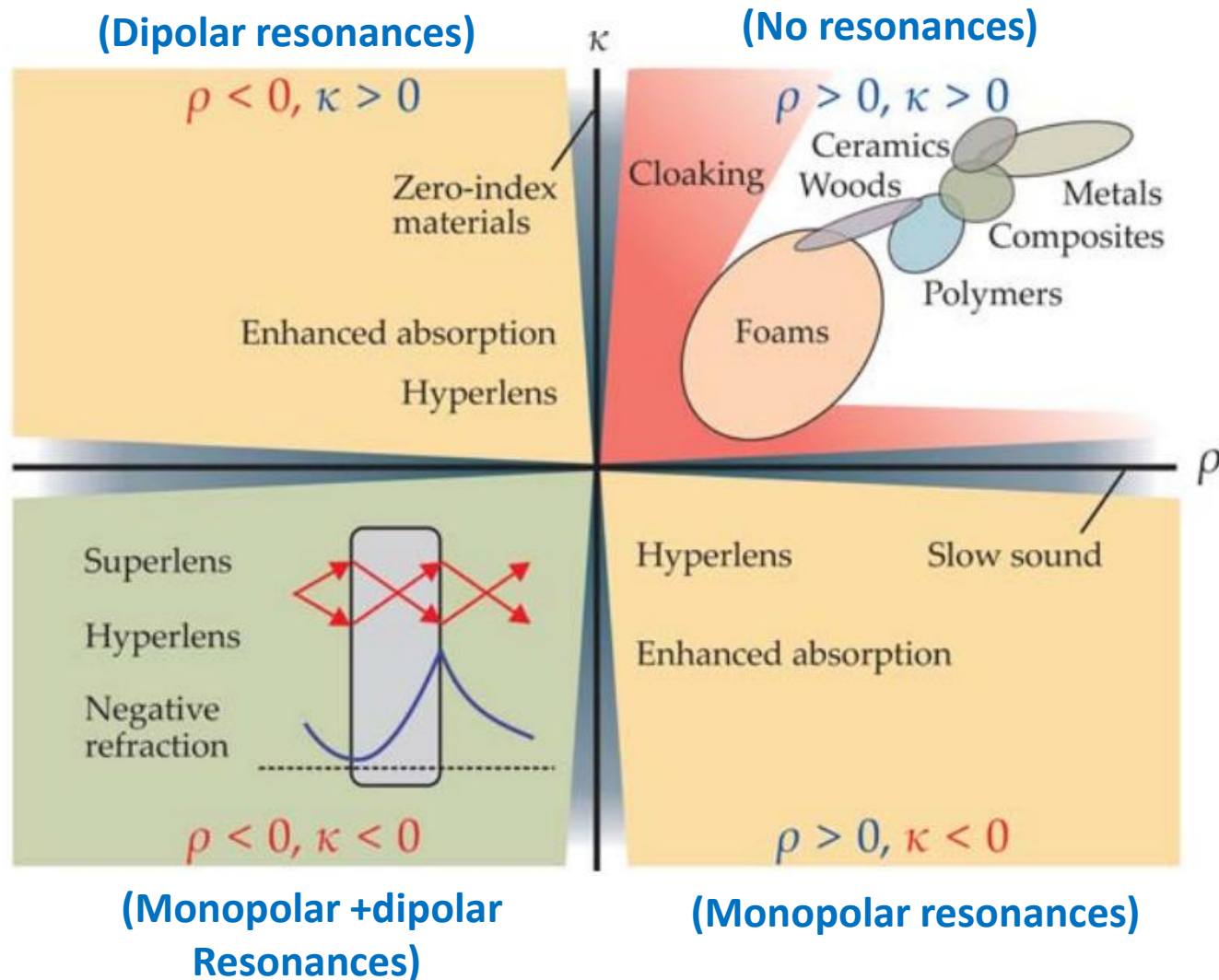
1. Introduction
2. Acoustic metamaterials with negative parameters
3. Visco-thermal effects in acoustic metamaterials with double-negative parameters
4. Sound absorption and redirection with sonic crystals based on metamaterial units

Acoustic metamaterials / metafluids

Acoustic metamaterials are artificial structures made of subwavelength units such that their **acoustic properties** are **NEW** in comparison with that of the building units



Acoustic metamaterials



$$c = \sqrt{\frac{\kappa}{\rho}}$$

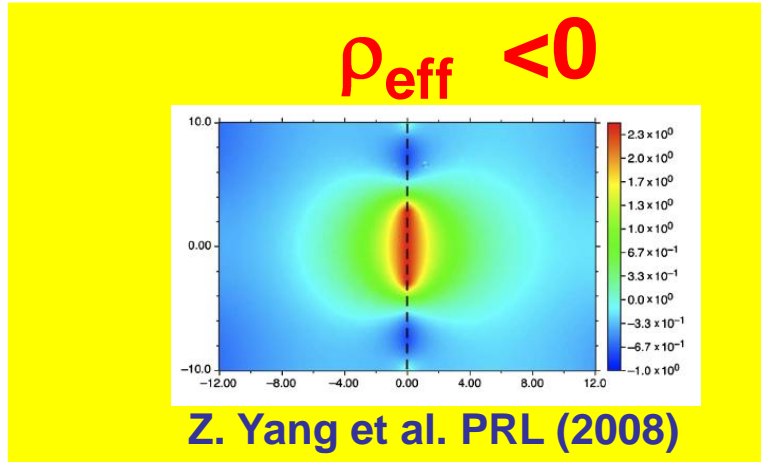
κ : bulk modulus
 ρ : density
 c : speed of sound

METAgenierie2017, 2-7 July.

Li and Chan, PRE (2004)

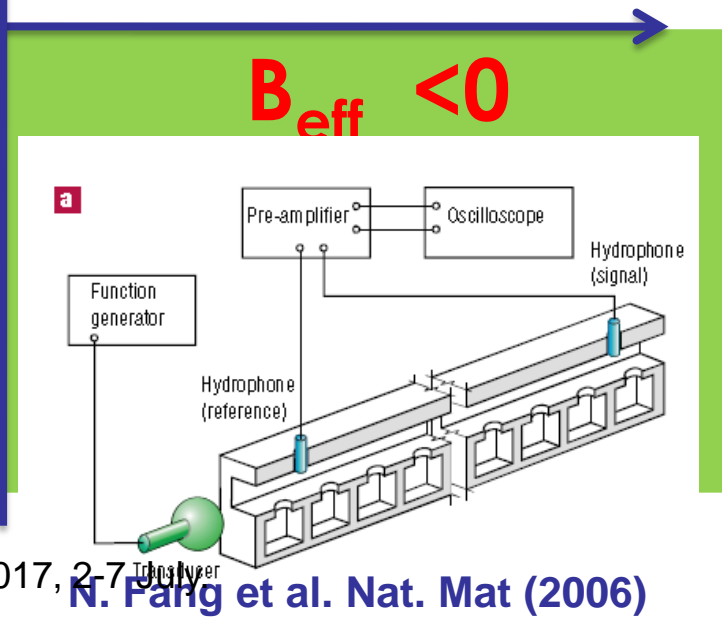
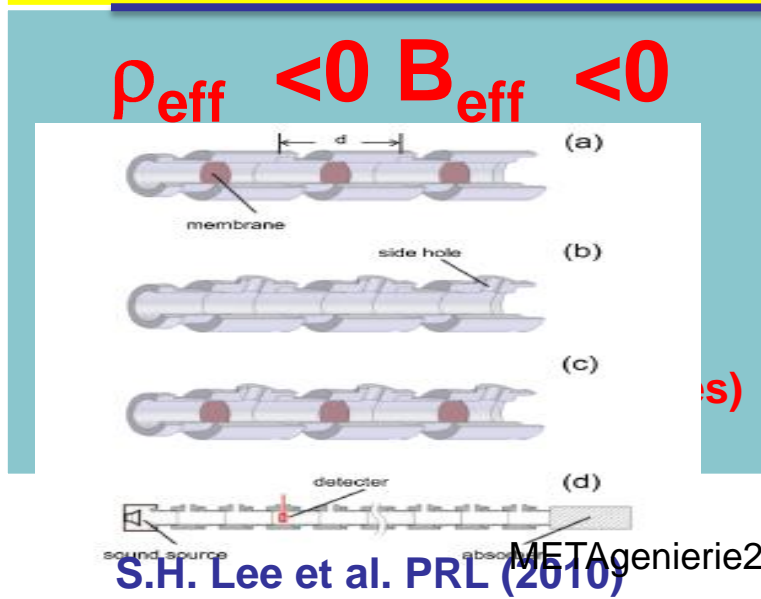
Acoustic metamaterials / Metafluids

B_{eff}



$\rho_{\text{eff}} > 0$
 $B_{\text{eff}} > 0$

(No resonances)



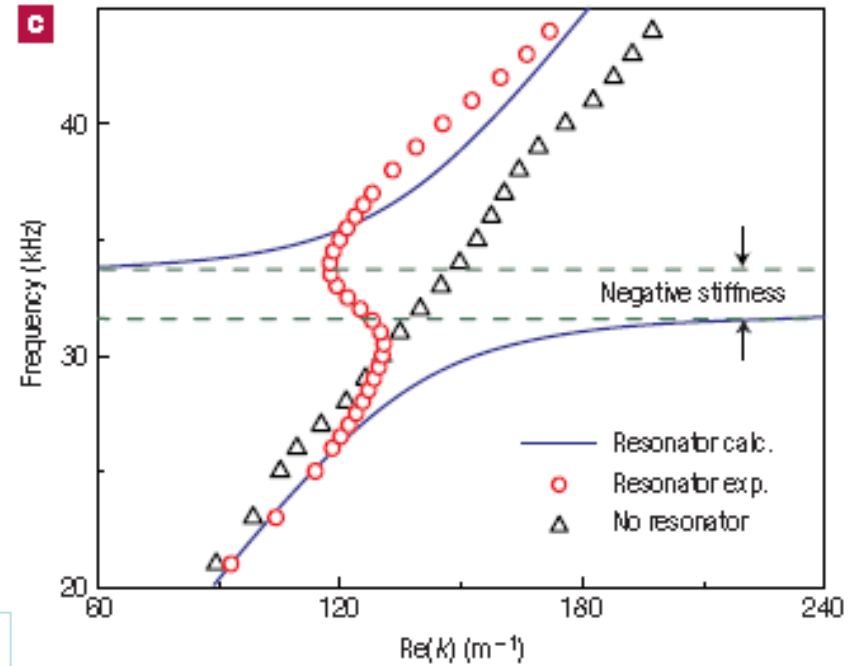
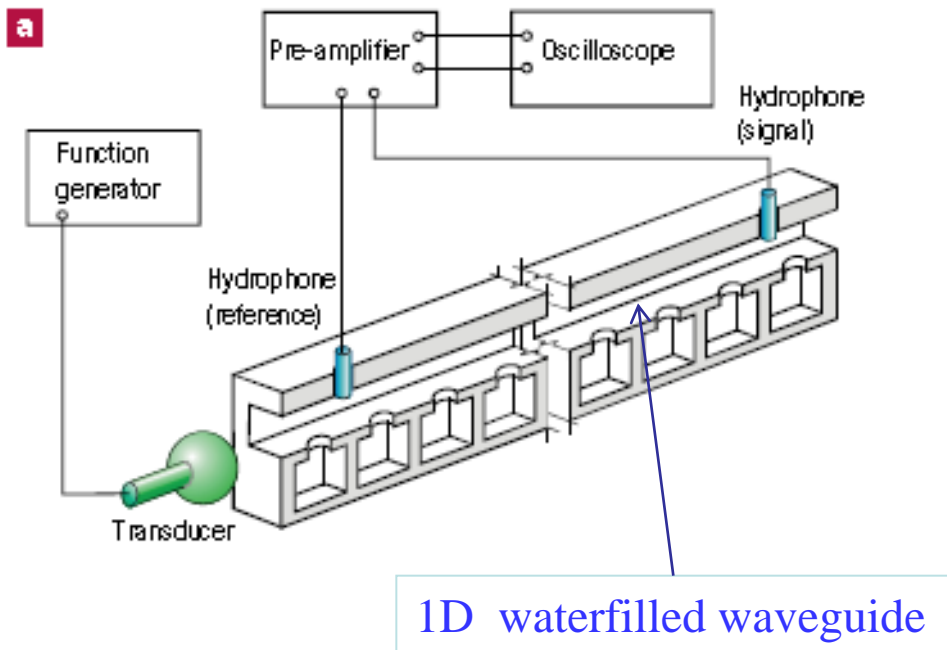
Recent Results on Acoustic metamaterials

OUTLINE

1. Introduction
2. Acoustic metamaterials with negative parameters
3. Visco-thermal effects in double-negative acoustic metamaterials
4. Sound redirection and splitting based on metamaterial units

INTRODUCTION: metamaterials with negative bulk modulus

N. Fang et al., *Ultrasonic metamaterials with negative bulk modulus*, Nat. Mat. 5, 452 (2006)



Effective modulus:

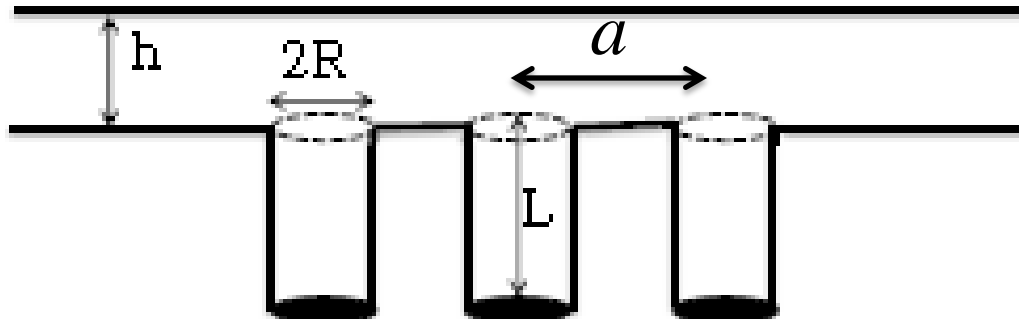
$$E_{\text{eff}}^{-1}(\omega) = E_0^{-1} \left[1 - \frac{F\omega_0^2}{\omega^2 - \omega_0^2 + i\Gamma\omega} \right], \text{ where } \Gamma \text{ is the dissipation loss in the HR:}$$

METAgenierie2017, 2-7 July.

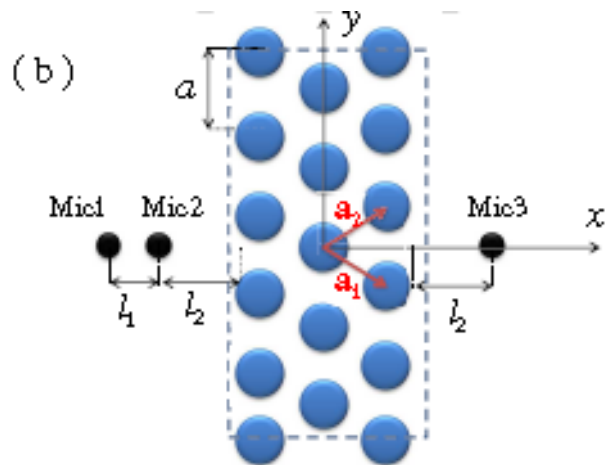
$$\Gamma = 2\pi \text{ 400Hz}$$

The quasi-2D metafluid

2D Waveguide (h) + cylindrical holes (R, L)



hexagonal lattice
with parameter a



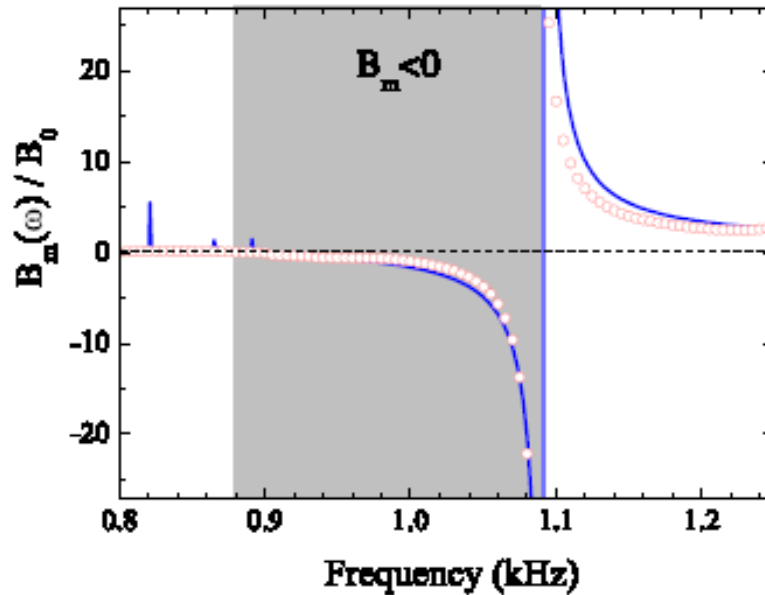
holes with $R=1\text{ cm}$, $L=9\text{ cm}$, $a=3\text{ cm}$
2D waveguide with $h=5\text{ cm}$



METAgenierie2017, 2-7 July.

Parameter extraction: theory vs experiment

Following Fokin et al, Phys. Rev. B, **76**, 144302 (2007)



From $R(\omega)$ and $T(\omega)$

$$B_m^{-1} = B_0^{-1} \left[1 - \frac{F\omega_0^2}{\omega^2 - \omega_0^2 + i\Gamma\omega} \right]$$

$$\omega_0 < \omega < \omega_0 \sqrt{1+F}$$

Parameters:

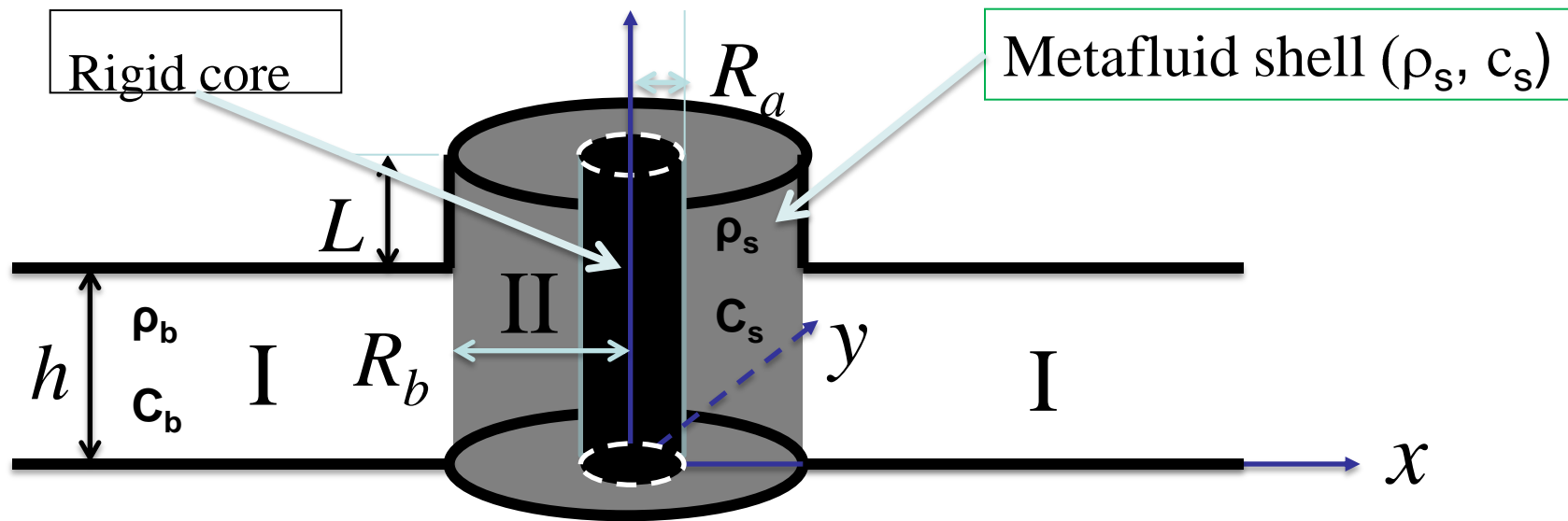
$$\omega_0 = 2\pi \times 874 \text{ Hz}$$

$$\Gamma = 2\pi \times 3.4 \text{ Hz}$$

METAgenierie2017, 2-7 July.

García-Chocano et al., Phys. Rev. B, **85**, 184102 (2012)

Double negative MtM: building unit



- **Pressure Field In the Region I**

$$P^I(r, \theta, z; w) = \sum_{q,n} [A_{qn} J_q(K_n^I r) + B_{qn} H_q(K_n^I r)] \Phi_n^I(z) \exp(iq\theta) \quad K_n^I = \sqrt{\left(\frac{w}{C_b}\right)^2 - \left(\frac{n\pi}{h}\right)^2}$$

- **Pressure Field in the Region II**

$$P^{II}(r, \theta, z; w) = \sum_{q,m} \left[C_{qm} J_q(K_m^{II} r) - \frac{j_q(K_m^{II} R_a)}{Y_q(K_m^{II} R_a)} Y_q(K_m^{II} r) \right] \Phi_m^{II}(z) \exp(iq\theta) \quad K_m^{II} = \sqrt{\left(\frac{w}{C_b}\right)^2 - \left(\frac{m\pi}{h+L}\right)^2}$$

Double negative metamaterial: T matrix approach

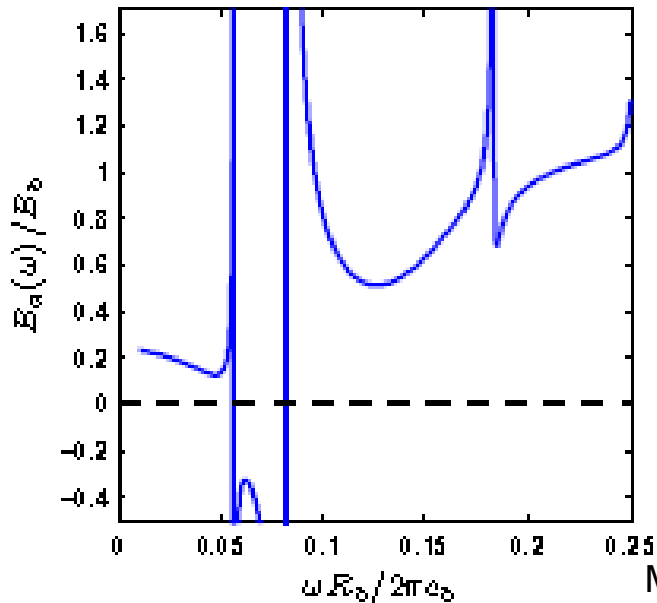
Torrent and JSD, New J. Phys., **13**, 093018 (2011)

Building unit: Metafluid cylinder with $c < c_{air}$

Bulk modulus: $B_a(\omega)$

$$\frac{B_a(\omega)}{B_b} = \frac{k_b^2 R_b^2}{2} \ln k_b R_b - \frac{1}{2} k_b R_b \chi_0$$

$$h=R_b \quad R_a=0.5R_b$$



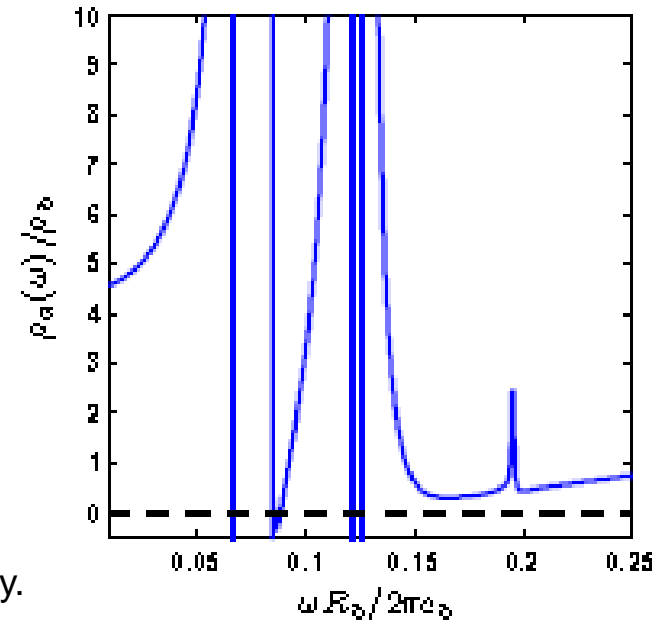
$$\rho_s = 2\rho_{air},$$

$$c_s = 0.3c_{air}$$

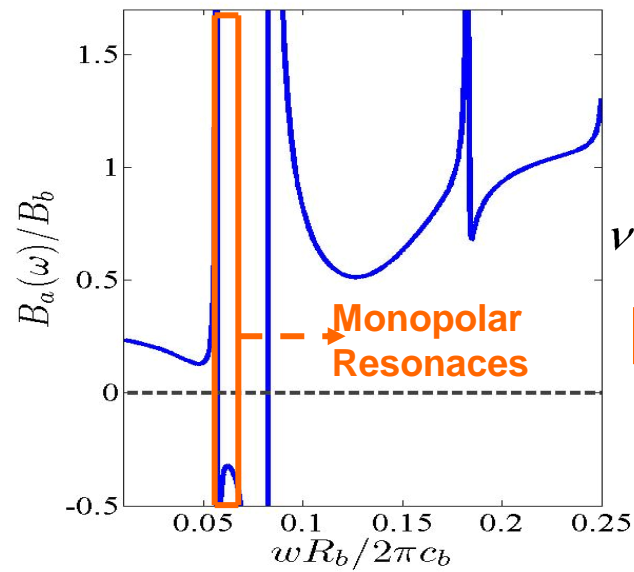
Mass density: $\rho_a(\omega)$

$$\frac{\rho_a(\omega)}{\rho_b} = \frac{\chi_1}{k_b R_b}$$

$$h=R_b \quad R_a=0.5R_b$$



MtM with negative parameters: resonant behavior of the building units

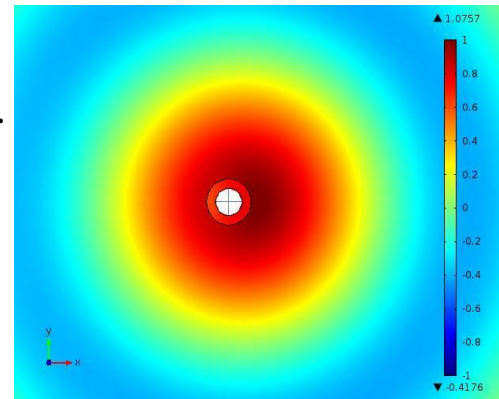


$\nu = 0.06u.r$

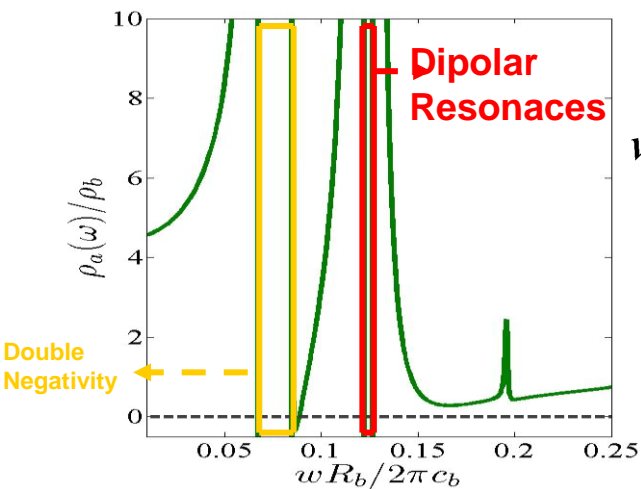
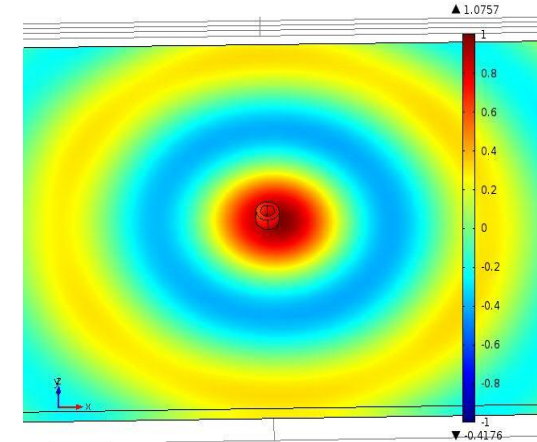


Scatter Pressure Field

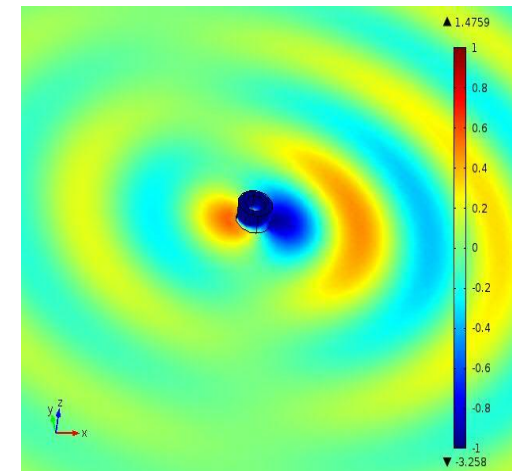
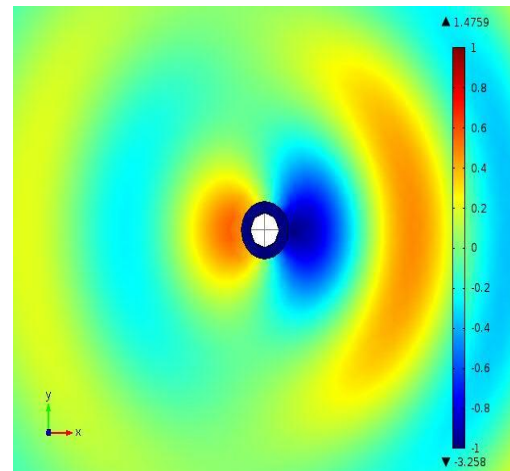
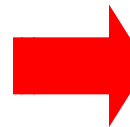
Plane XY view



3D view



$\nu = 0.12u.r$

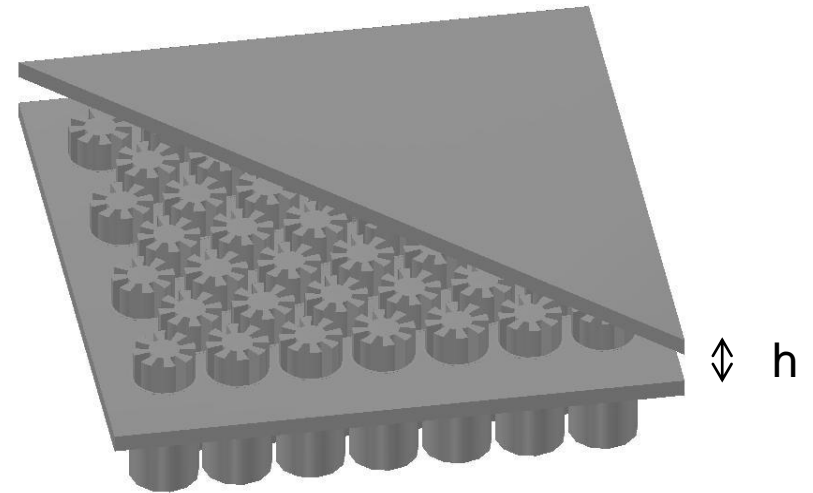


METAgenierie2017, 2-7 July.

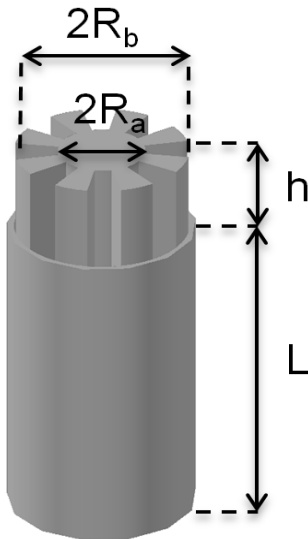
Graciá-Salgado, Torrent and JSD, NJP **14**, 103052 (2011)

Quasi-2D structure for double negative and $\rho \approx 0$ (DNZ) behavior

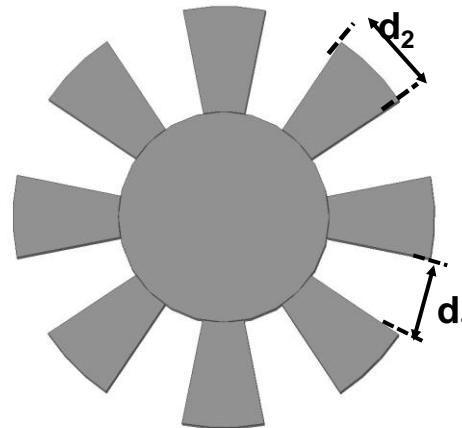
Scheme of the artificial structure



Building unit



Transversal section

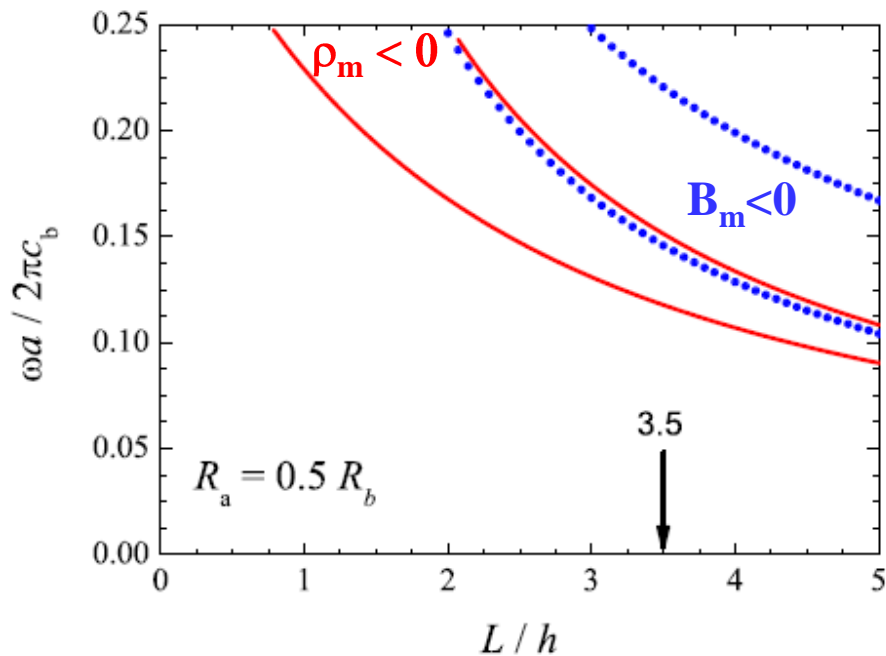


$$\rho_s = \frac{d_1 + d_2}{d_2} \rho_b = 2\rho_b$$

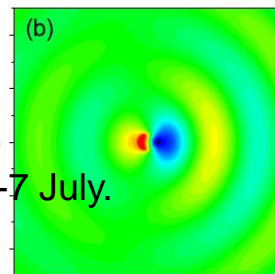
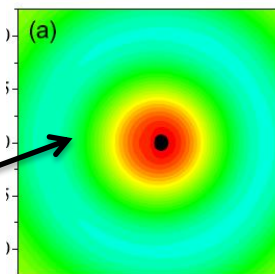
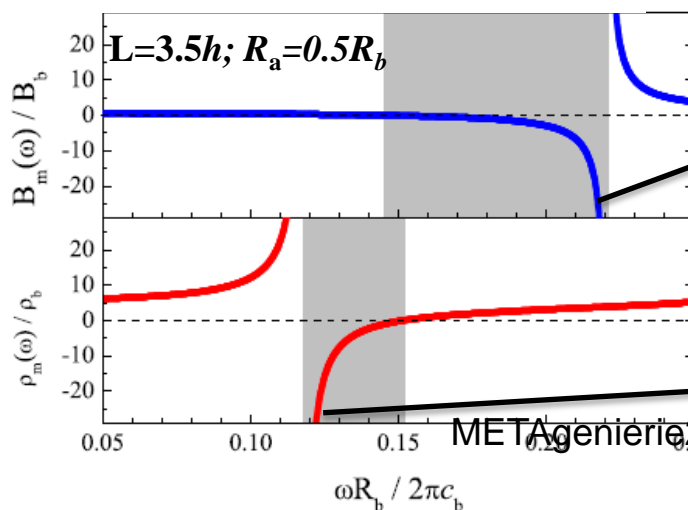
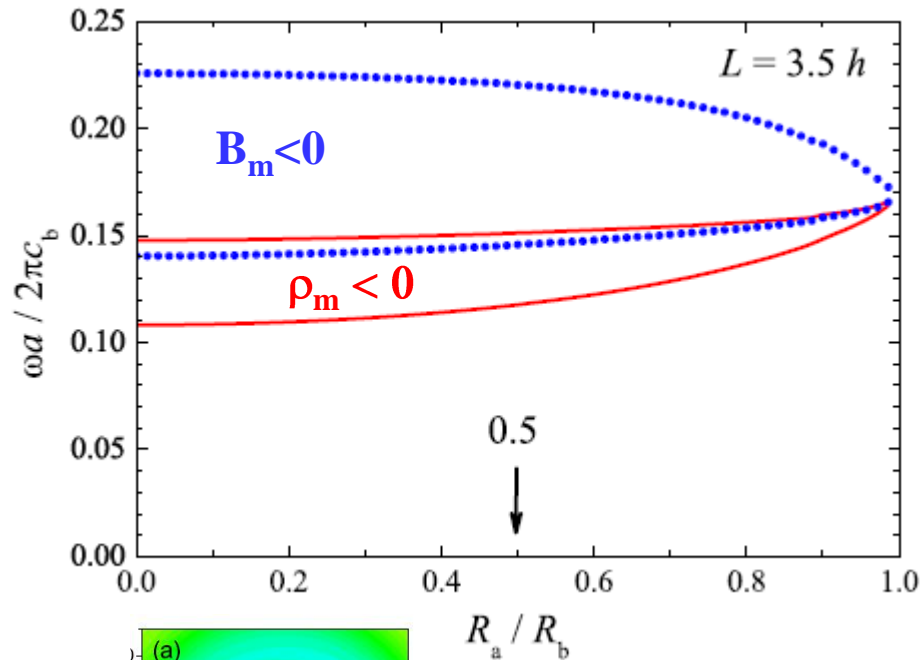
Spiouzas et al., APL (2011)

Quasi-2D structure for double negative and DNZ behavior

ω - L Phase diagram



ω - R_b Phase diagram



J. Li and C.T. Chan,
PRE(2004)

ρ -near-zero (DNZ) metamaterials

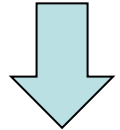
$$\rho_m < 0 \approx 0; B_m < 0$$



$$c_m = \sqrt{\frac{B_m}{\rho_m}} \rightarrow \infty$$



$$n_m \approx 0$$

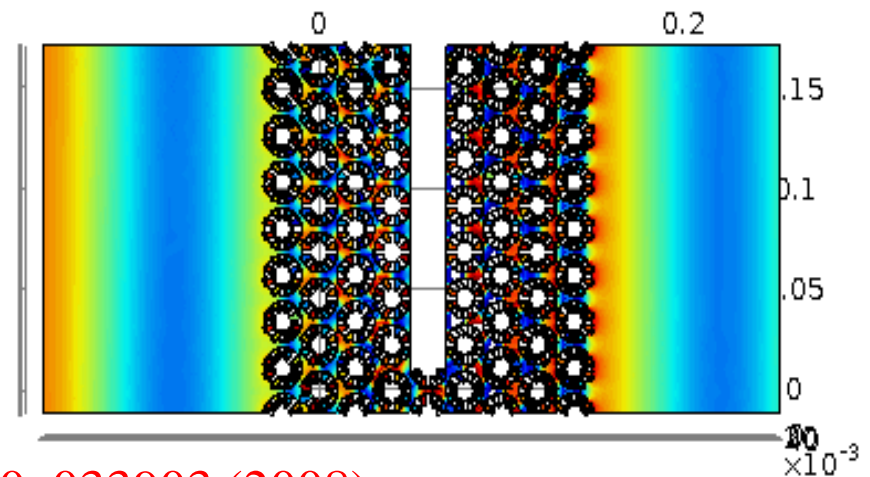
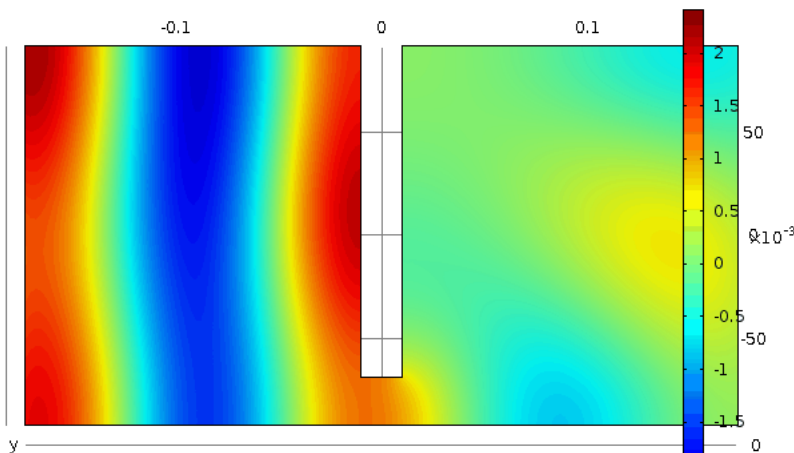


$$|Z_m|^2 = \rho_m B_m \approx \rho_b B_b = |Z_b|^2$$

Surface: Pressure (Pa)

$$e^{ik_m x} \approx 1$$

Transmission through narrow channels $\lambda \gg a$



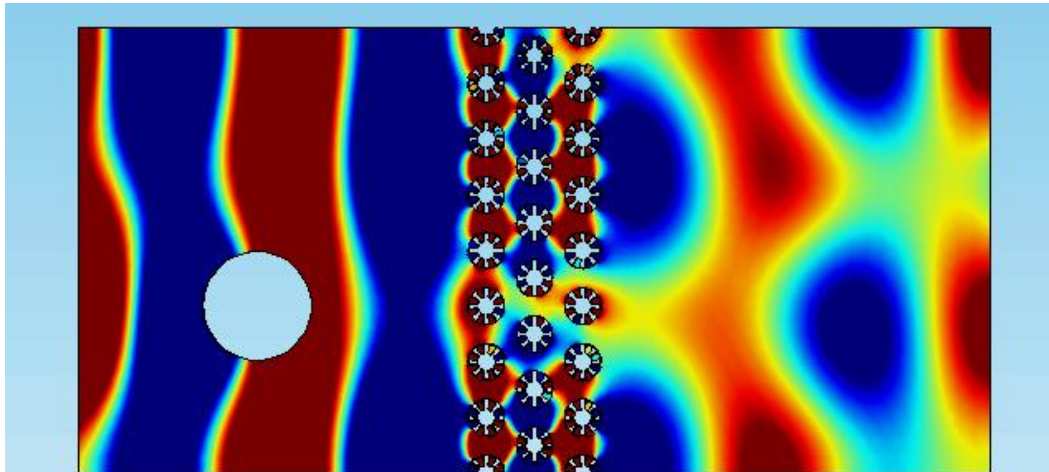
EM counterpart: Edwards *et al.*, PRL 100, 033903 (2008)

METAgenierie2017, 2-7 July.

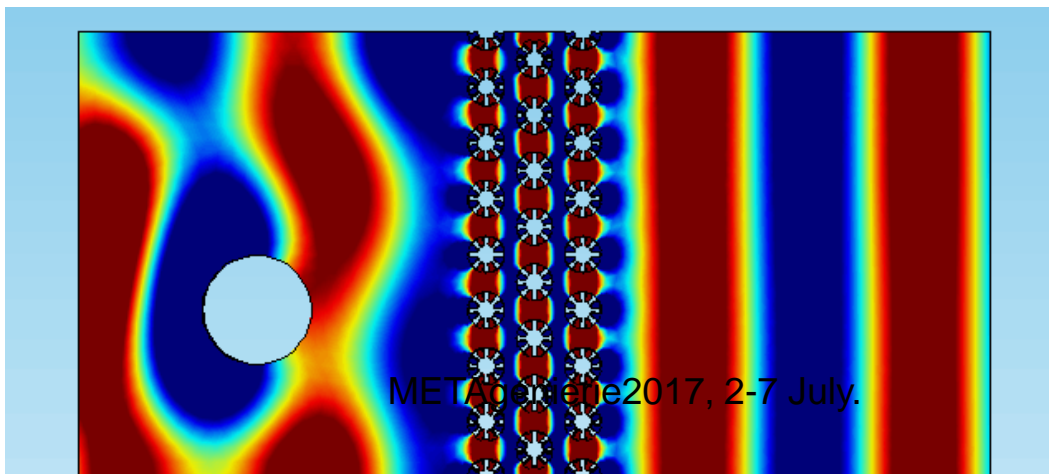
Liu *et al.*, PRL 100, 023903 (2008)

Applications of DNZ metamaterials: control of the radiation pattern

Scattering by a rigid cylinder + MtM slab
(both embedded in a 2D waveguide)

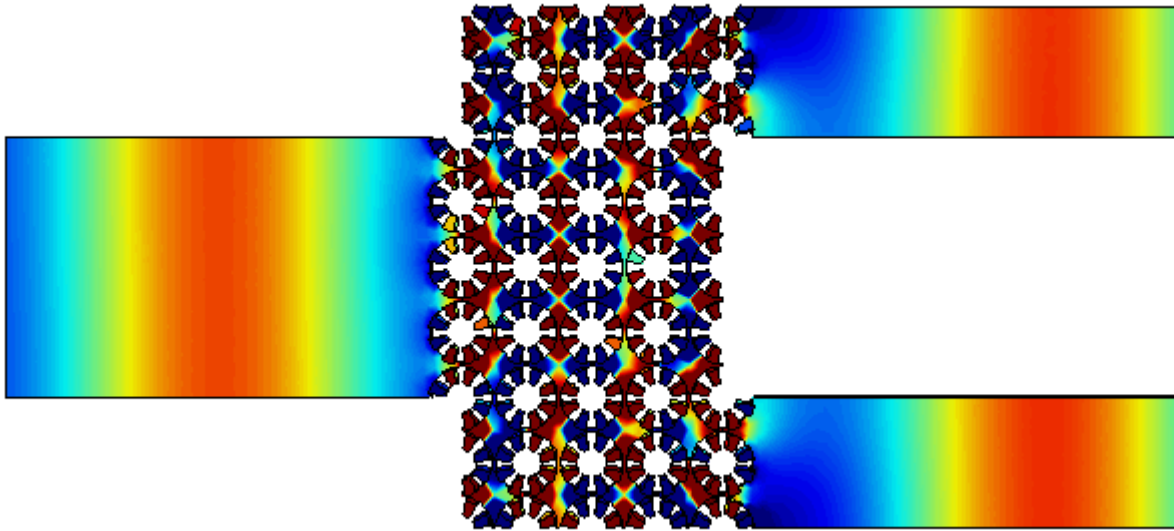


Scattering at the frequency where the MtM behaves as a ρ -near-zero material

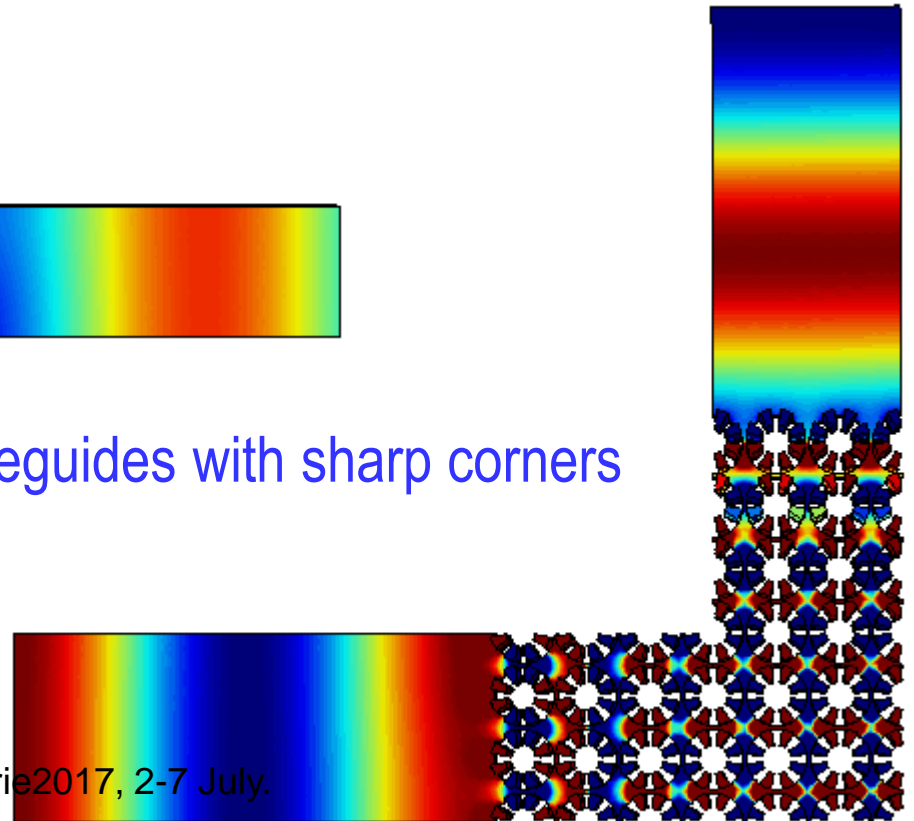


Applications of DNZ metamaterials:

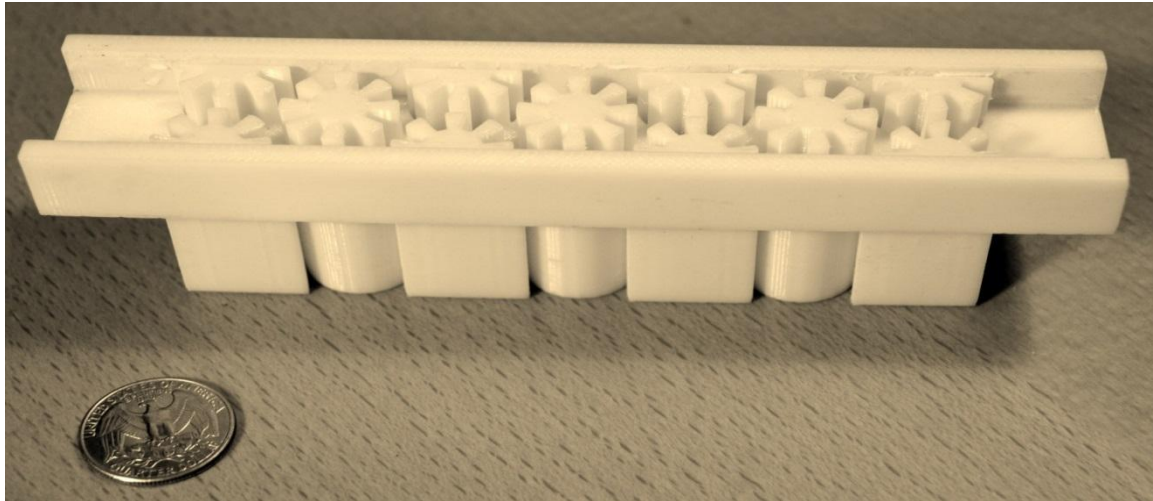
- Power splitter



- Perfect transmission through waveguides with sharp corners



Quasi-2D acoustic metamaterials: Practical realization



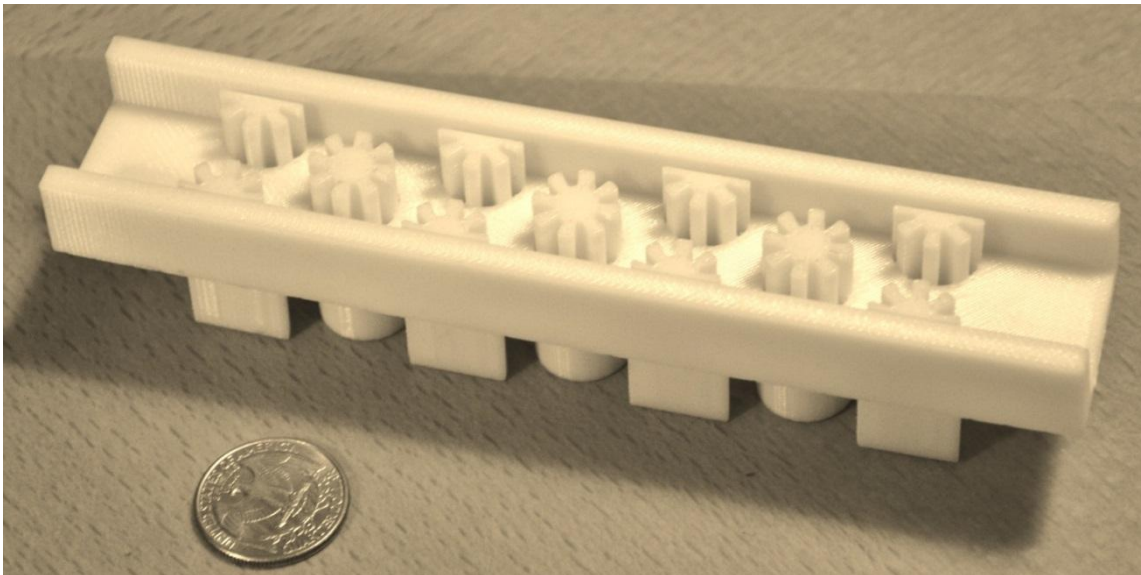
Sample A

$$a=21 \text{ mm}$$

$$R_b=9.2\text{mm}$$

$$h=9\text{mm}$$

$$L=3.5h$$



Sample B

$$a=21 \text{ mm}$$

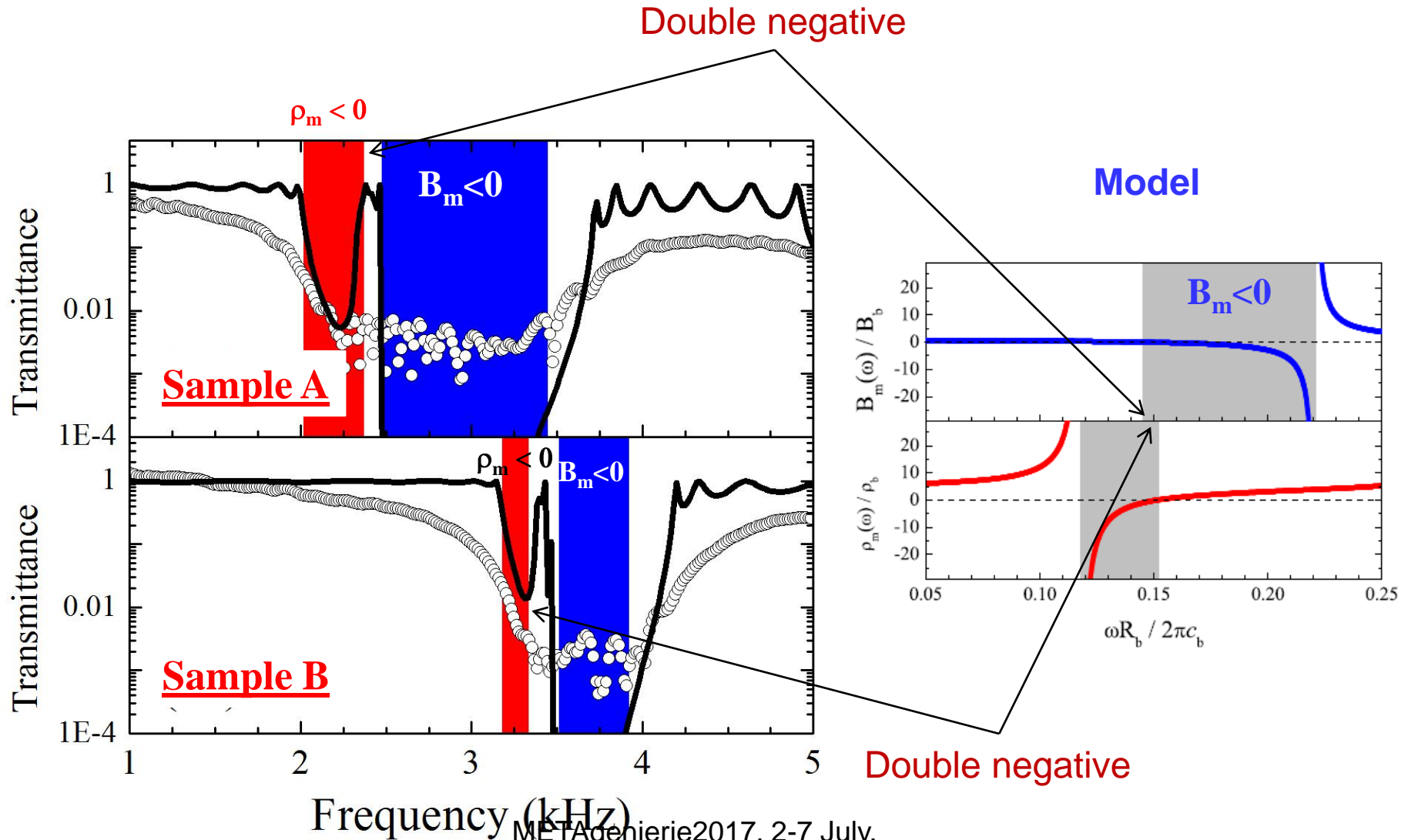
$$R_b=7\text{mm}$$

$$h=9\text{mm}$$

$$L=2.5h$$

Quasi-2D acoustic metamaterials: Practical realization

Experimental characterization



METAgenierie2017, 2-7 July.

Gracia-Salgado *et al.*, Phys. Rev. B **88**, 224305 (2013)

Acoustic metamaterials

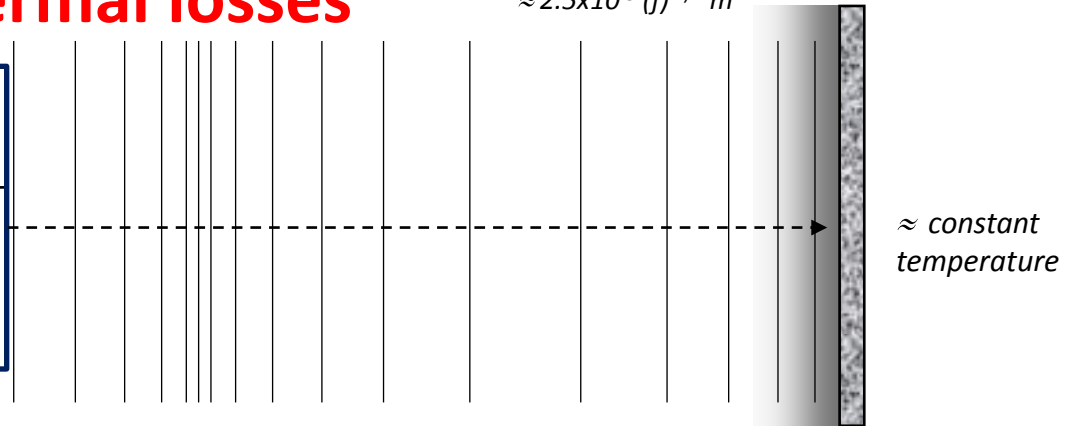
OUTLINE

1. Introduction
2. Acoustic metamaterials with negative mass density and density near zero
3. Visco-thermal in acoustic metamaterials with double-negative parameters
4. Sound redirection and splitting with sonic crystals based on metamaterial units

Thermal losses

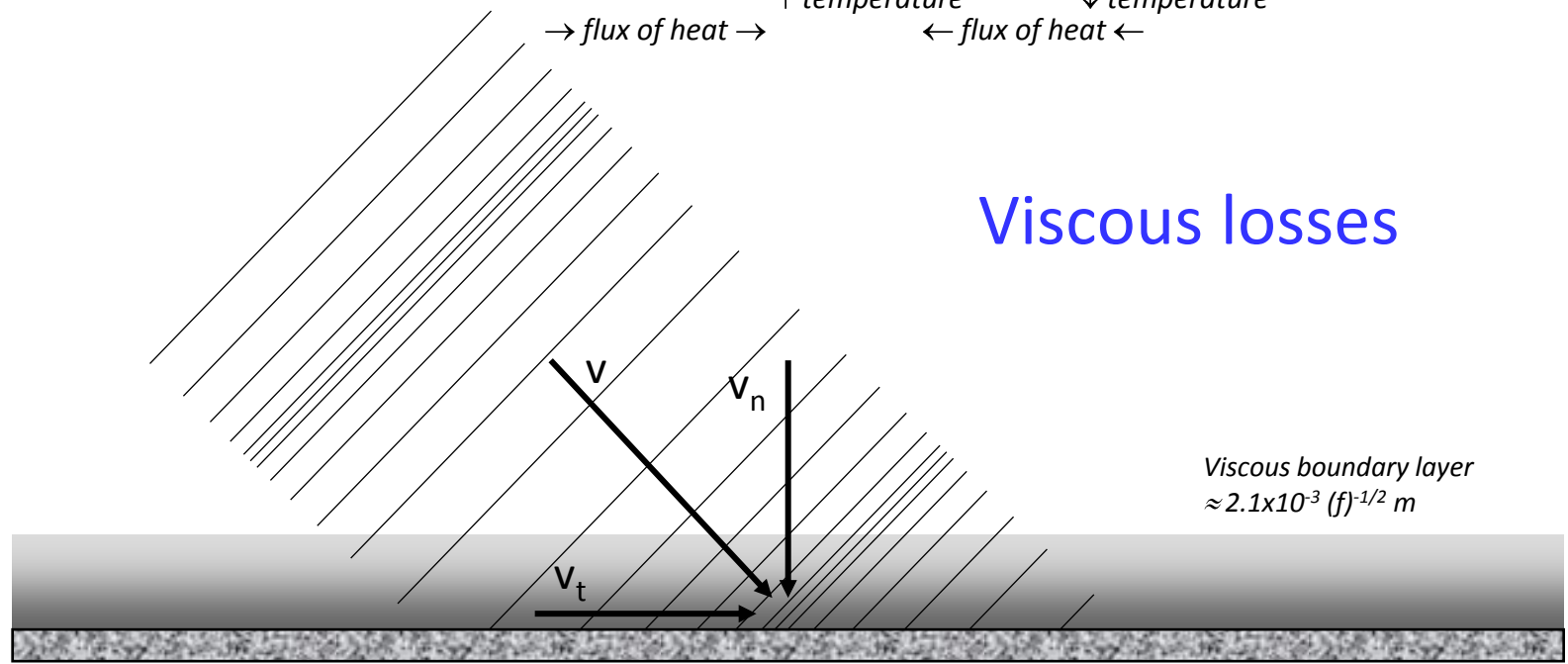
Thermal boundary layer
 $\approx 2.5 \times 10^{-3} (f)^{-1/2} \text{ m}$

f (Hz)	viscous layer (μm)	thermal layer (μm)
100	210	250
1000	66	79
10000	21	25
20000	15	16



\uparrow pressure \downarrow pressure
 \uparrow temperature \downarrow temperature
 \rightarrow flux of heat \rightarrow \leftarrow flux of heat \leftarrow

Viscous losses



$V_t = 0$ at the boundary

METAgénierie2017, 2-7 July.

Viscous and thermal losses

Linearized Navier-Stokes model:

- Conservation of mass:

$$\frac{\partial \rho}{\partial t} + \rho_o \nabla \cdot \vec{v} = 0$$

- Conservation of energy:

$$\rho_o T_o \frac{\partial s}{\partial t} = \lambda \Delta T$$

- Conservation of momentum (Navier-Stokes equation):

$$\rho_o \frac{\partial \vec{v}}{\partial t} = -\nabla p + \left(\eta + \frac{4}{3} \mu \right) \nabla (\nabla \cdot \vec{v}) - \mu \nabla \times (\nabla \times \vec{v})$$

- Thermodynamic equations:

$$s = \frac{C_p}{T_o} \left(T - \frac{\gamma - 1}{\beta \gamma} p \right)$$

$$\rho = \frac{\gamma}{c^2} p - \beta T$$

Numerical methods for Visco-Thermal losses

Low reduced frequency model (LRFM):

- Neglects pressure variation and velocity component in the direction normal to the boundary. Restricted to some geometries

Finite Element Method (FEM) implementation:

- Direct implementation of the linearized Navier-Stokes equations. No restricting assumptions.

Boundary Element Method (BEM) implementation:

- Uses Kirchhoff's decomposition of the linearized N-S equations. No restricting assumptions.

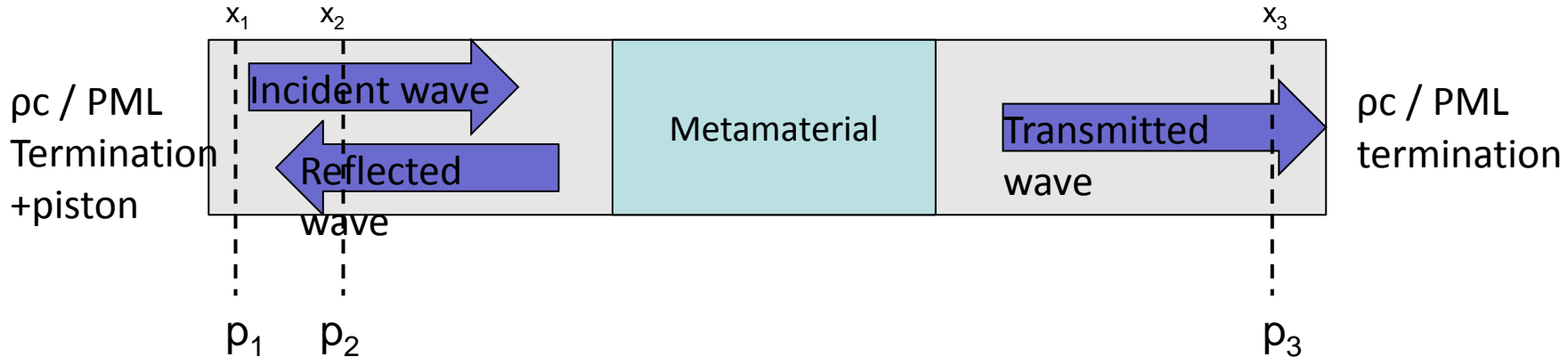
Time/Load	SW package
Fast/Low	ACTRAN, ANSYS, COMSOL
Slow/High	COMSOL
Slow/High	OpenBEM (non-commercial)

LRFM: W. M. Beltman. *Viscothermal wave propagation including acousto-elastic interaction. Part I: Theory and Part II: Applications.* J. Sound Vib. 227 (3), 1999.

FEM: M. Malinen, M. Lyly, P. Råback, A. Kärkkäinen and L. Kärkkäinen. *A finite element method for the modeling of thermo-viscous effects in acoustics.* Proc. 4th ECCOMAS, Jyväskylä, Finland, 1-12, 2004.

BEM: V. Cutanda Henriquez, P.M. Juhl, *An axisymmetric boundary element formulation of sound wave propagation in fluids including viscous and thermal losses*, JASA 134(5), 2013.
V. Cutanda Henriquez, P.M. Juhl, *Implementation of an Acoustic 3D BEM with Visco-Thermal Losses*, Internoise 2013, Innsbruck, Austria.

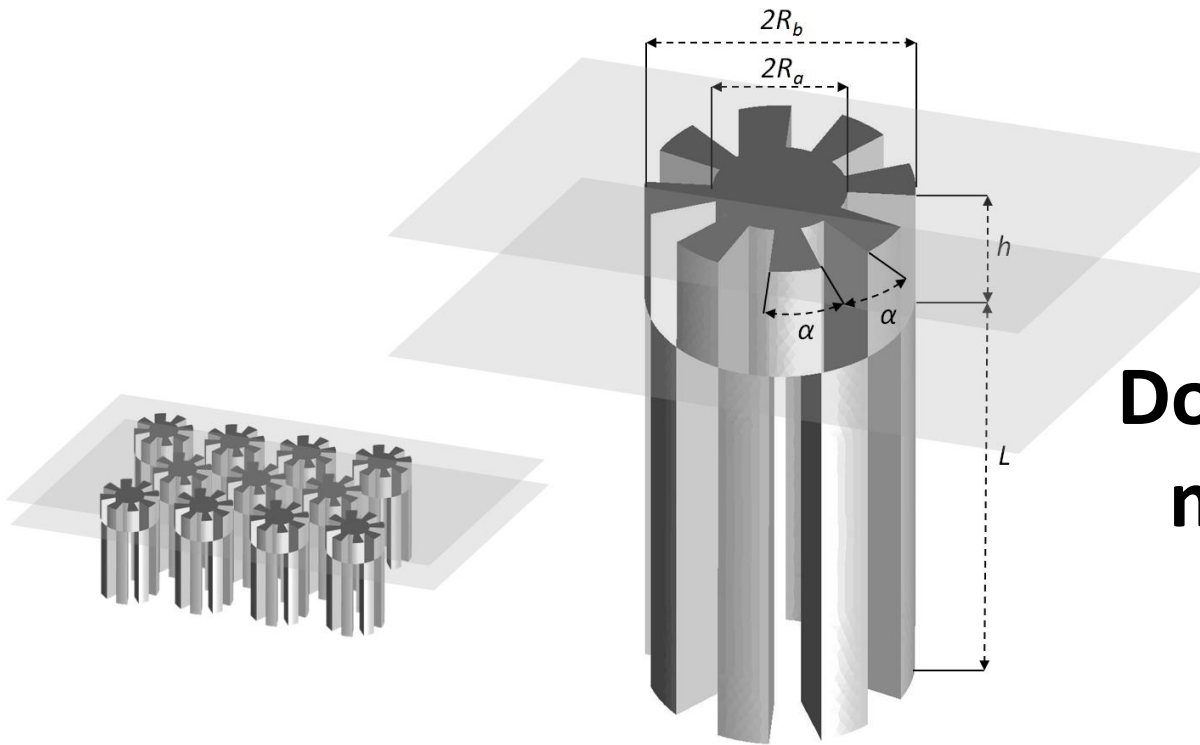
Metamaterial: transmission and reflection



Three-point method: Reflection and transmission coefficients:

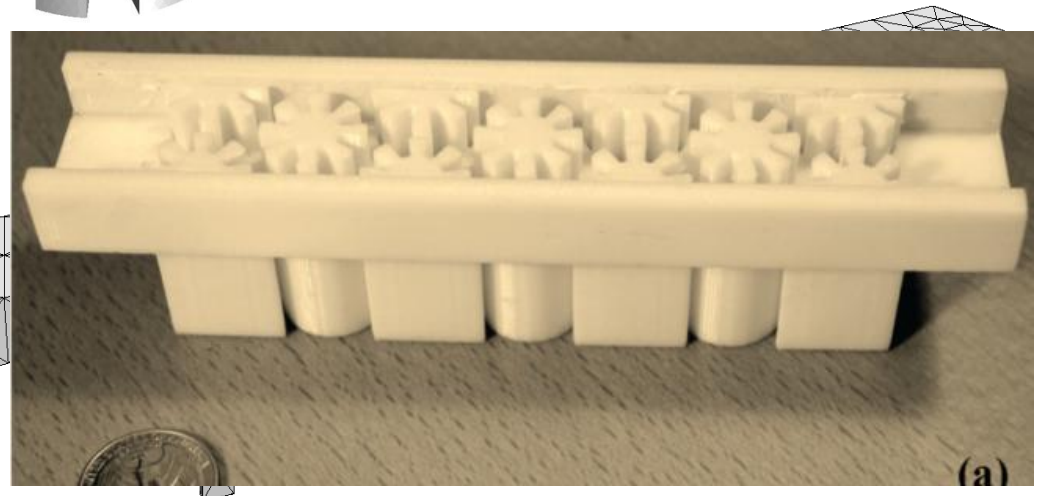
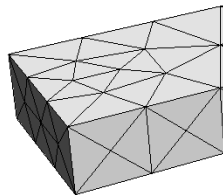
$$R(\omega) = \frac{p_2 e^{-ikx_1} - p_1 e^{-ikx_2}}{p_1 e^{-ikx_2} - p_2 e^{-ikx_1}} \quad T(\omega) = \frac{p_3}{p_2} \frac{e^{-ikx_2} + R(\omega) e^{ikx_2}}{e^{-ikx_3}} e^{-ik(x_2 - x_1)}$$

- Transmittance (fraction of transmitted power): $|T(\omega)|^2$
- Reflectance (fraction of reflected power): $|R(\omega)|^2$
- Absorbance (fraction of absorbed power): $1 - |T(\omega)|^2 - |R(\omega)|^2$



Double-negative metamaterial

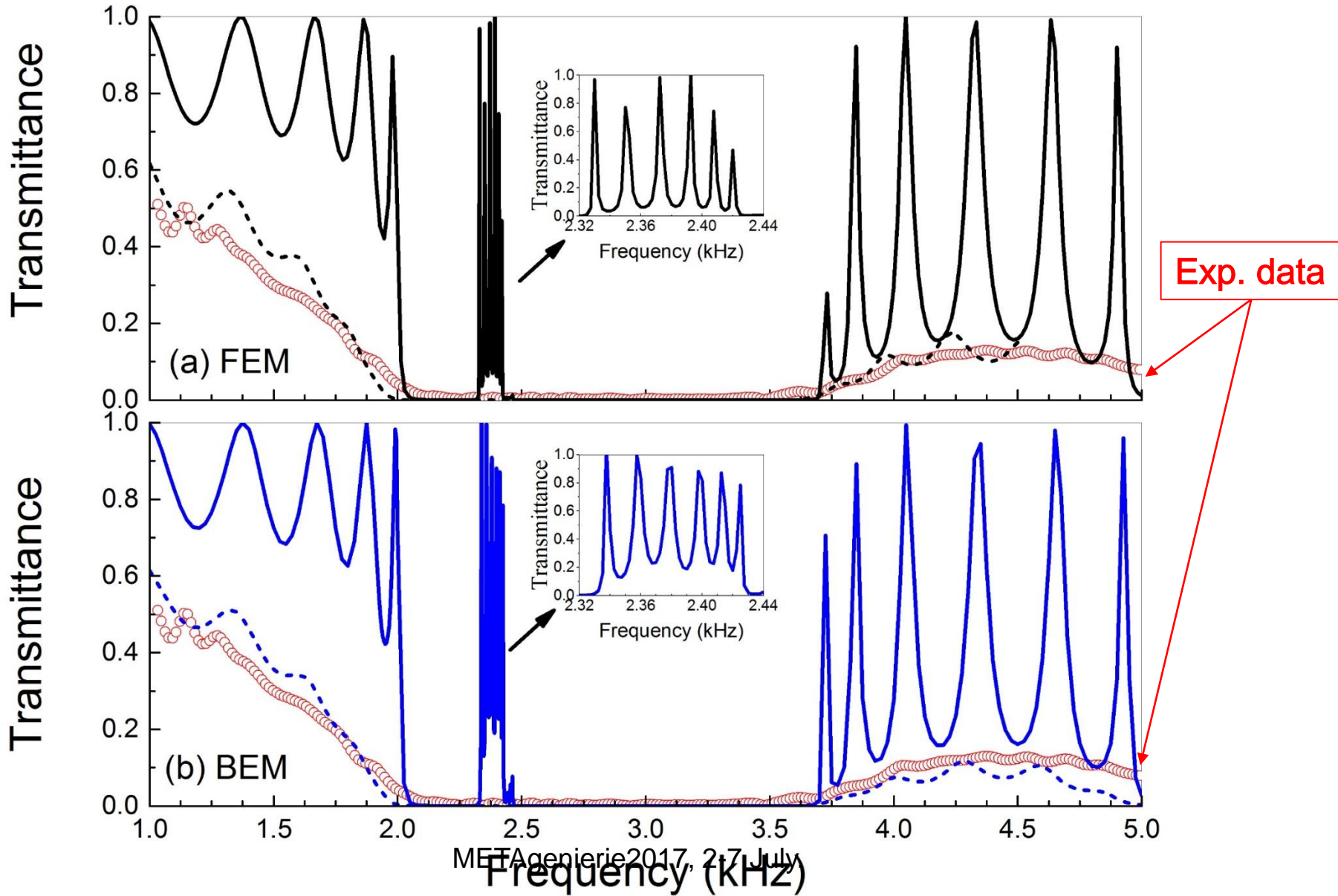
BEM: mesh with 4810 quadratic elements and 9616 nodes



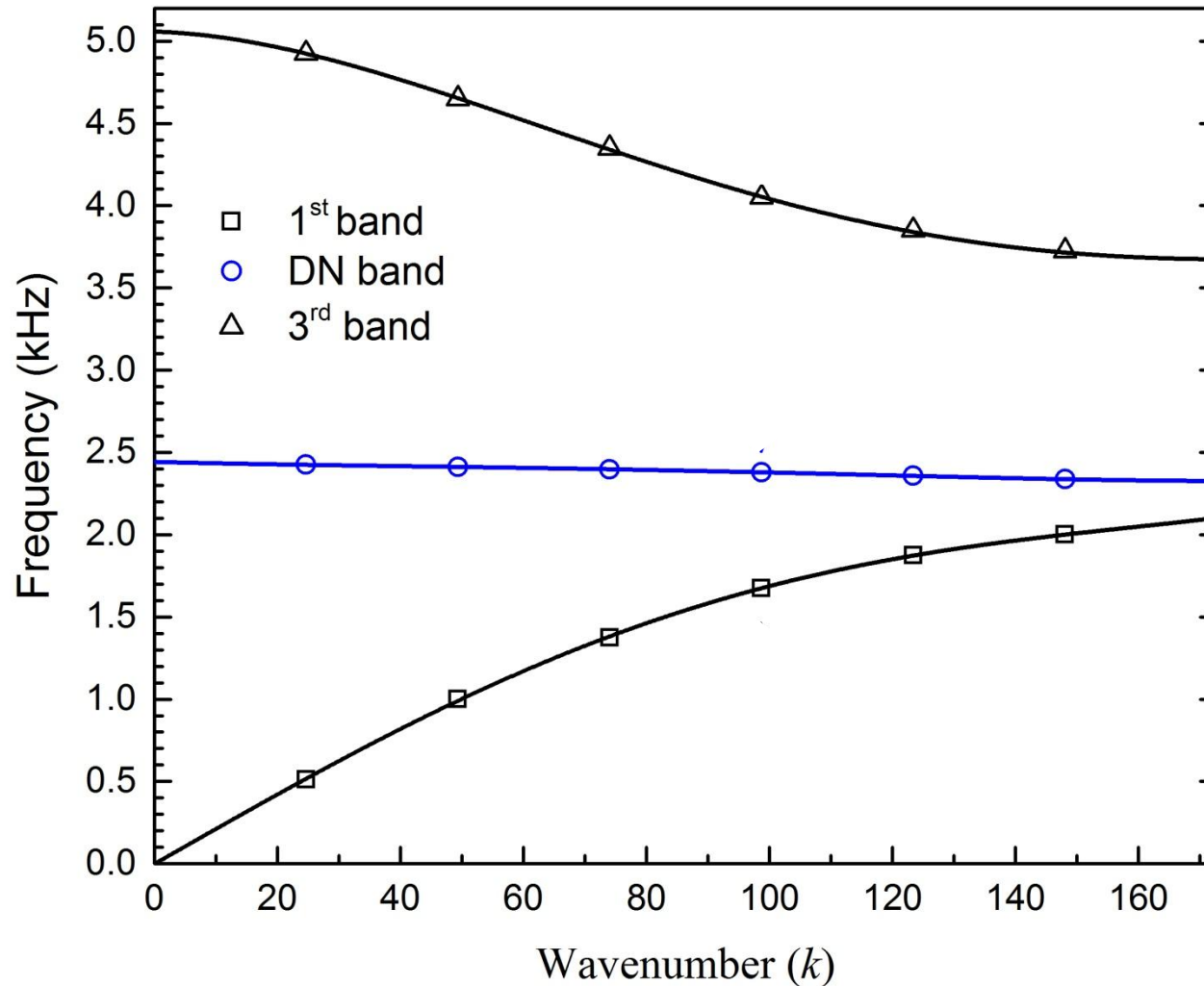
R. Graciá-Salgado, V. M. García-Chocano, D. Torrent, J. Sánchez-Dehesa, *Negative mass density and ρ -near-zero quasi-two-dimensional metamaterials: Design and applications*. *Physical Review B* **88**, 224305 (2013)

ME TAgénierie2017, 2-7 July.

FEM versus BEM

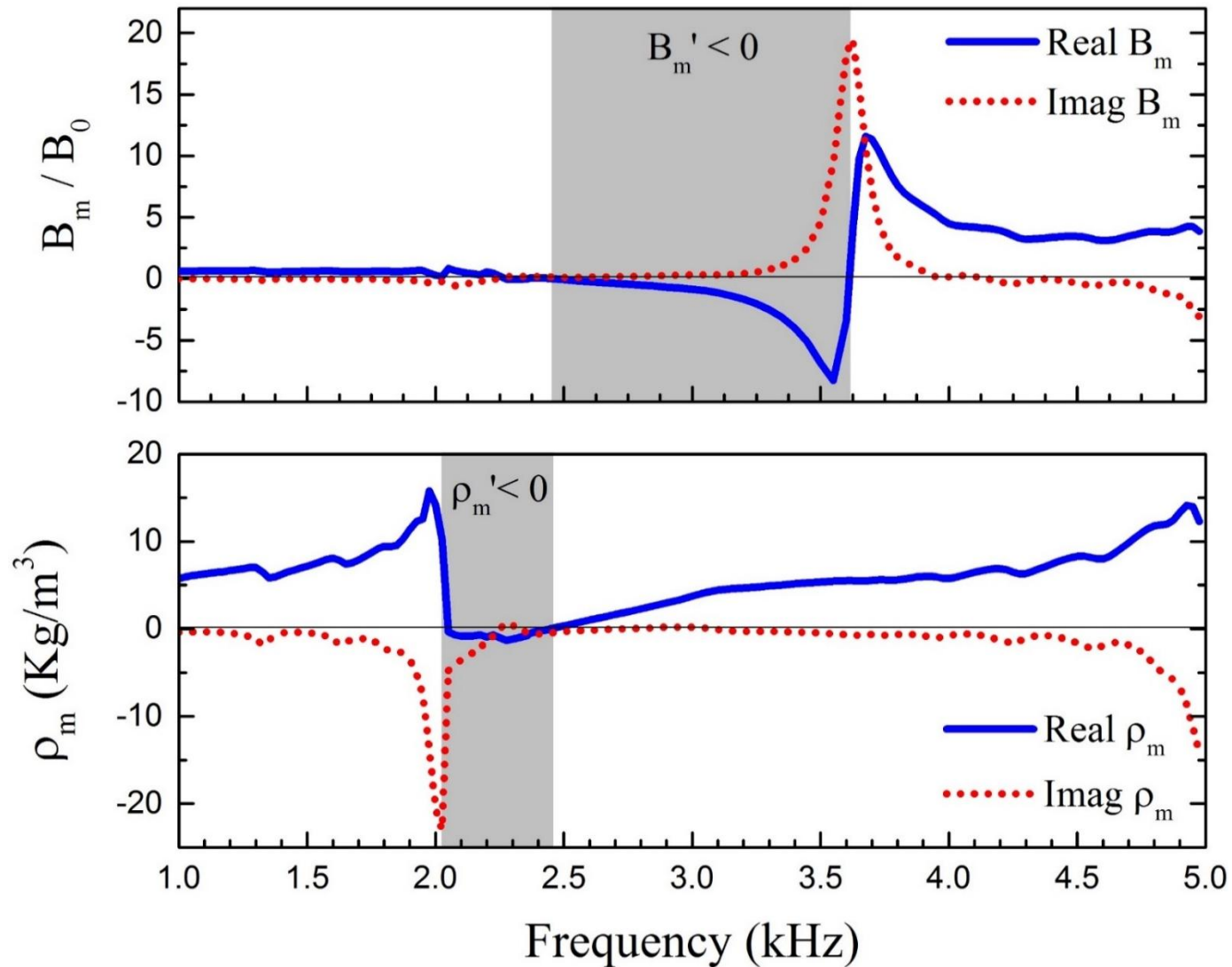


Acoustic band structure (no losses)



METAgenierie2017, 2-7 July.

Parameter extraction (with losses)

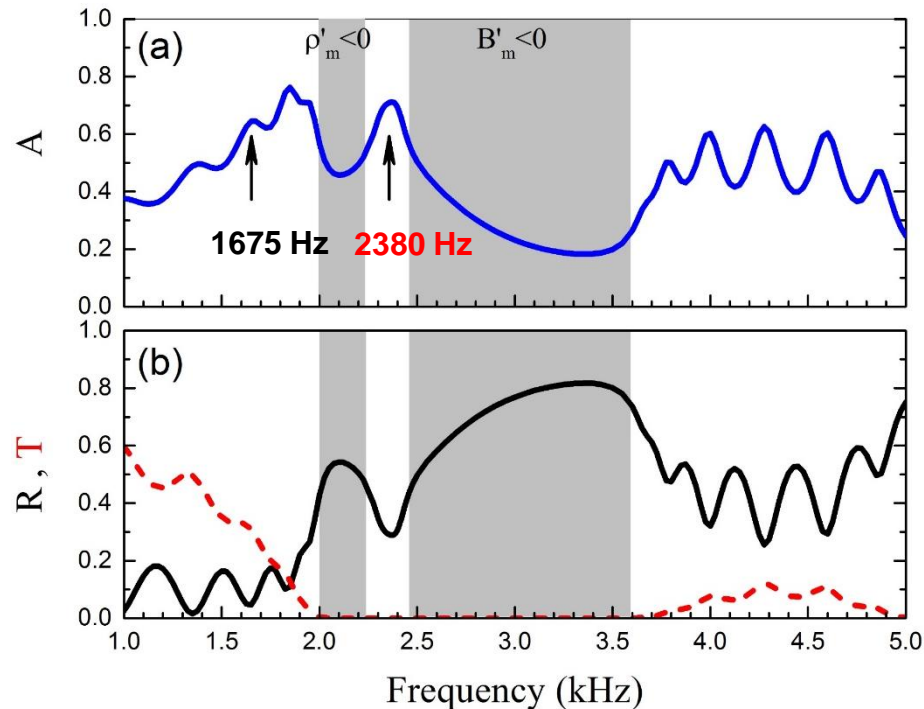


METAgenierie2017, 2-7 July.

Extracted from R and T, following the method of [Fokin *et al.*, PRB 77, 144302 \(2007\)](#)

Frequency dependence (with losses)

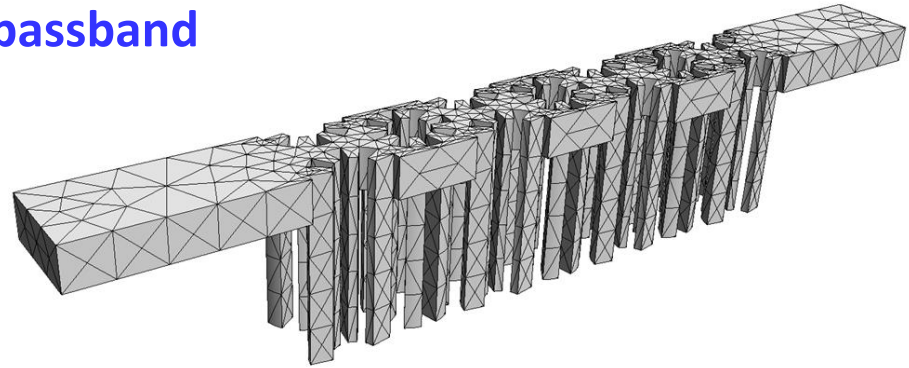
$$A=1-R-T$$



- Absorption in the first passband increases with decreasing v_g
- In the DN band there is a huge reflectance and almost a 100% of the transmitted energy is absorbed.

Double-negative metamaterial

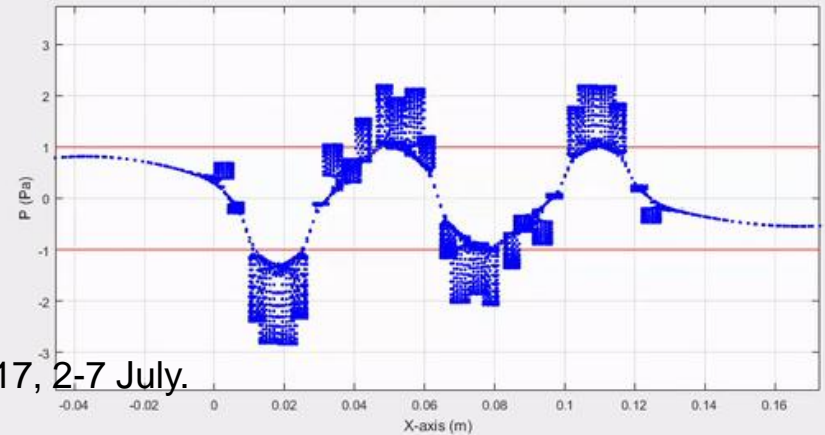
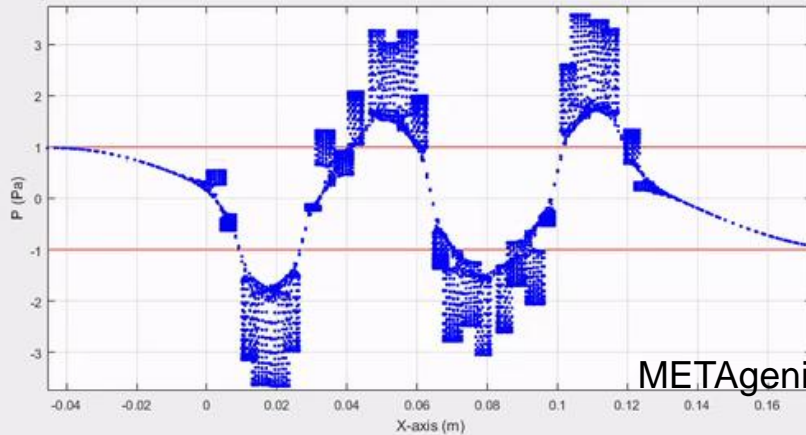
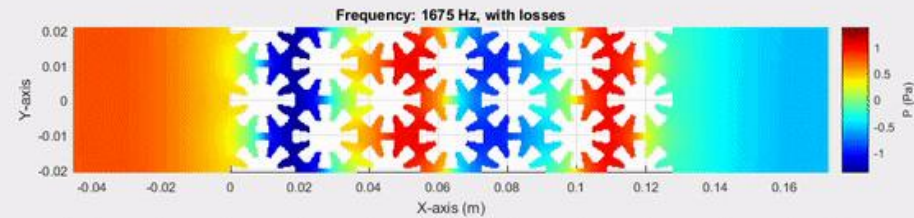
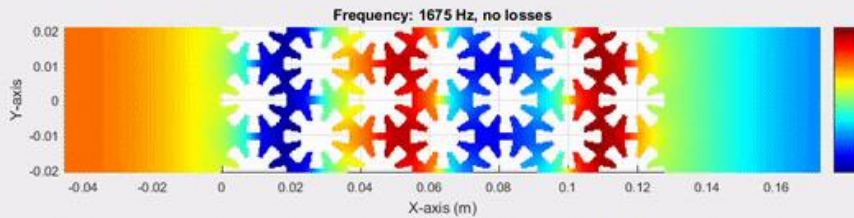
Visco-thermal effects on the first passband



$$f_{FP} = 1675 \text{ Hz}$$

No losses

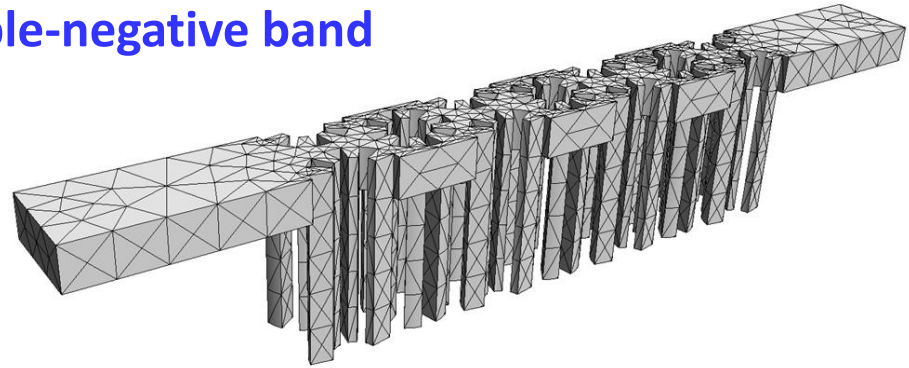
With losses



METAgenierie2017, 2-7 July.

Double-negative metamaterial

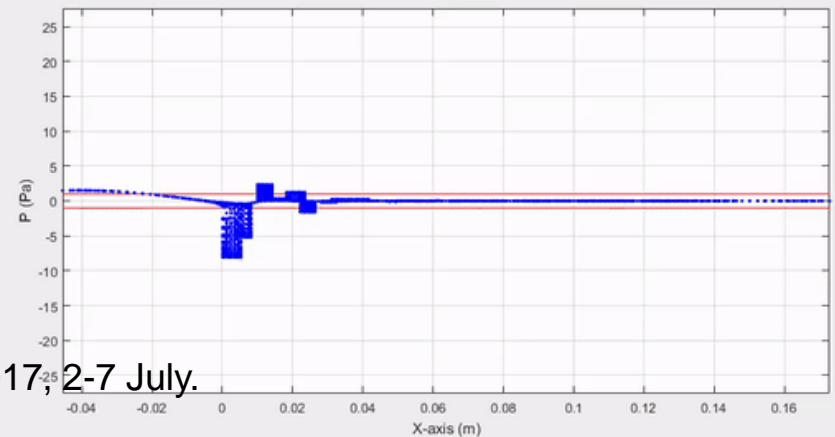
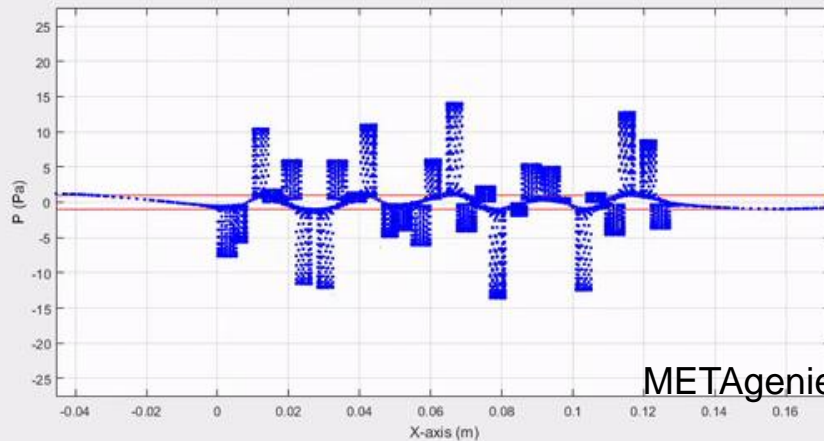
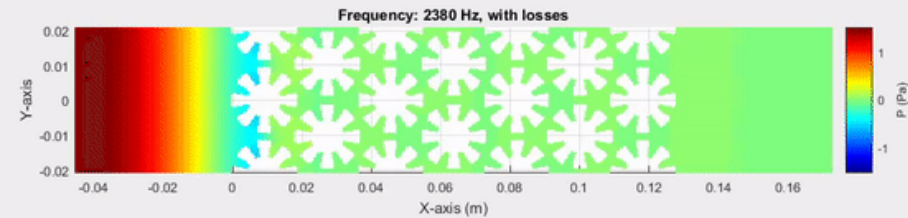
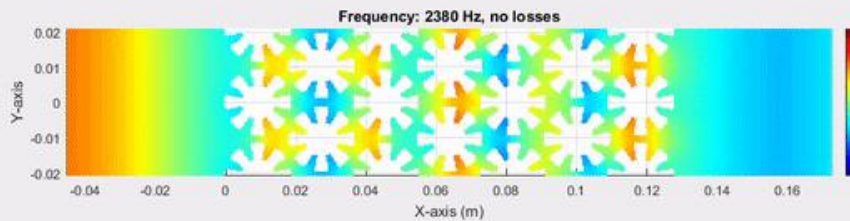
Visco-thermal effects on the double-negative band



$$f_{DN} = 2380 \text{ Hz}$$

No losses

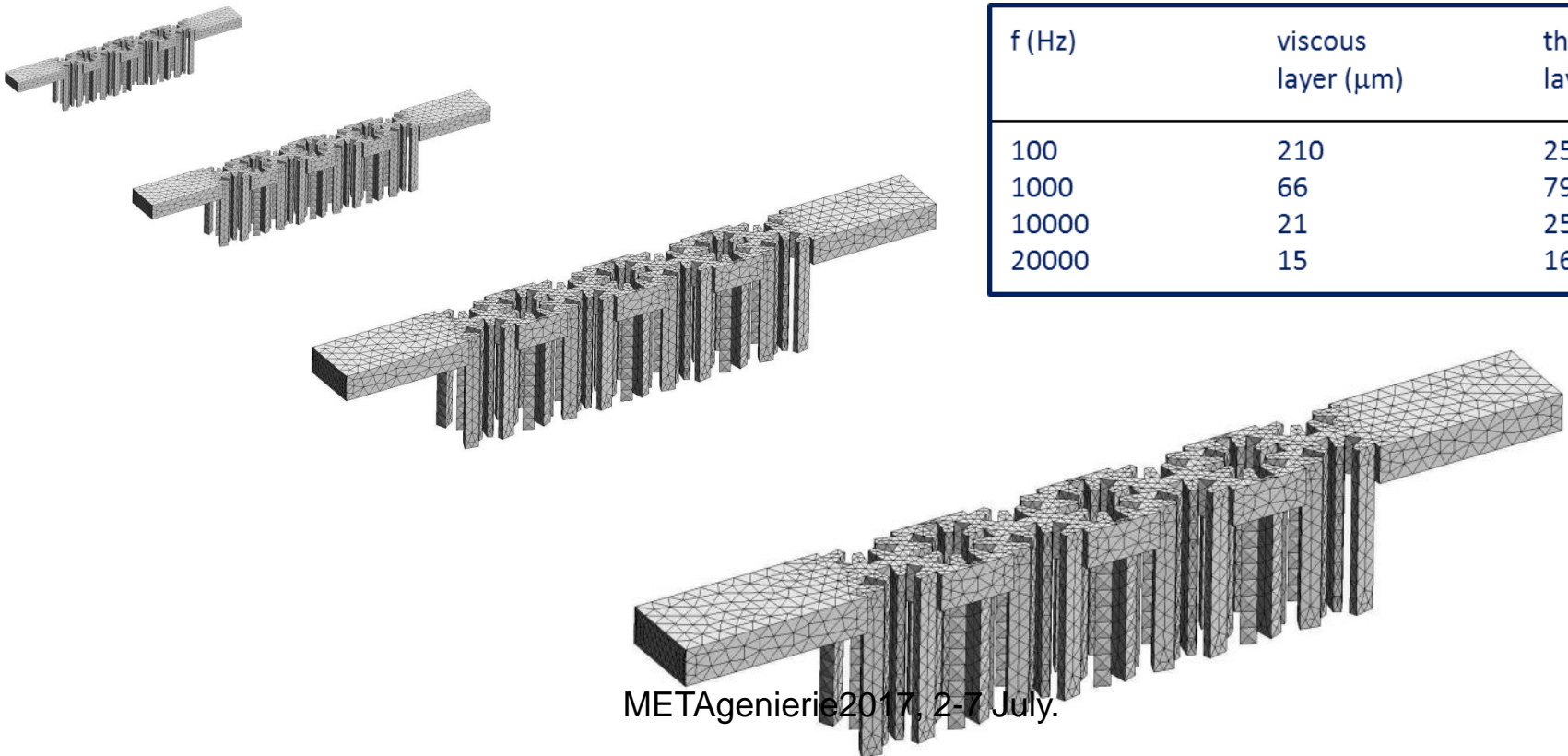
With losses



Scaling of the metamaterial

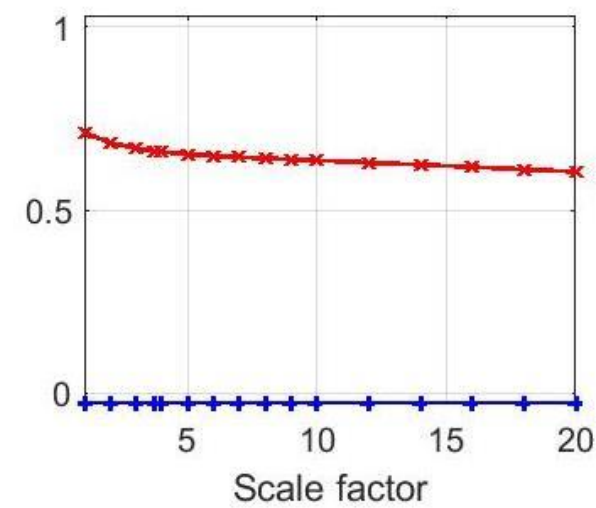
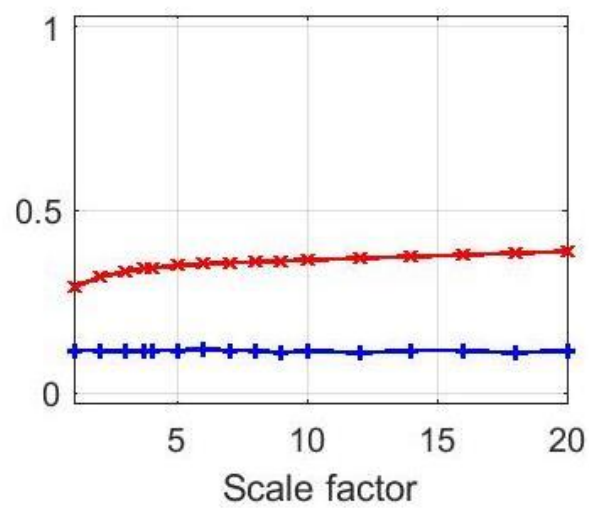
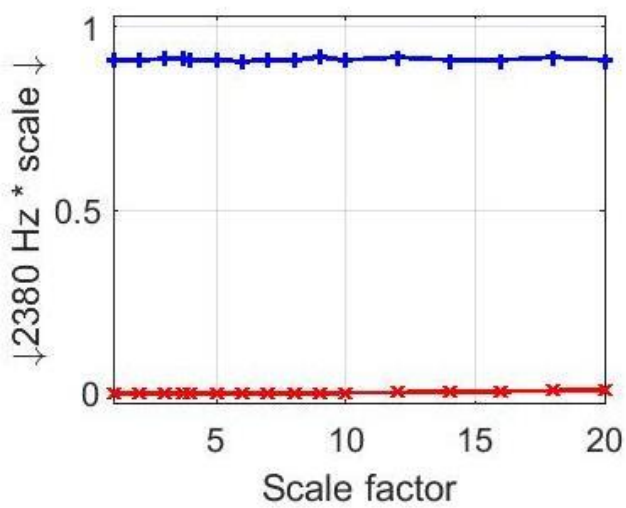
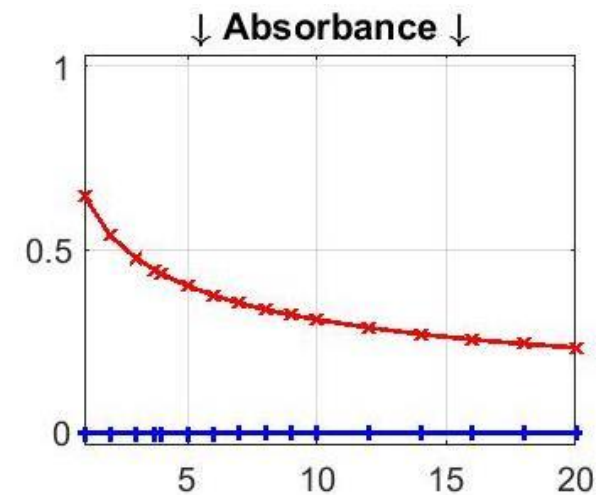
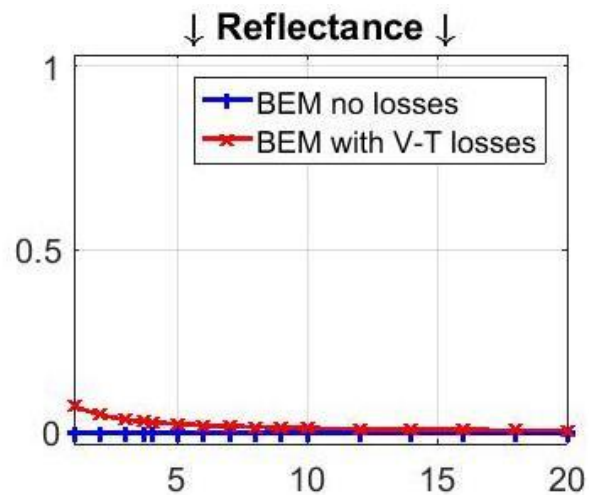
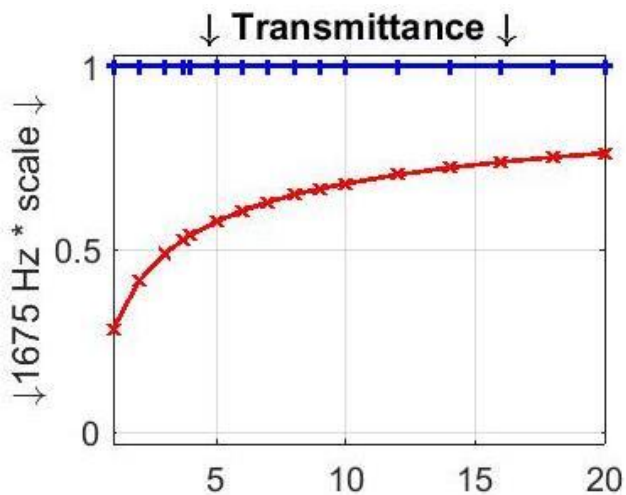
- As the size grows the frequency is scaled down: the **mesh can be reused**
- The behavior should be the same, **except for viscous and thermal losses (as $f^{-1/2}$)**:

$$\delta_v \approx \sqrt{\frac{2\nu}{\rho_0\omega}} \quad \delta_\kappa \approx \sqrt{\frac{2\kappa}{c_p\rho_0\omega}}$$

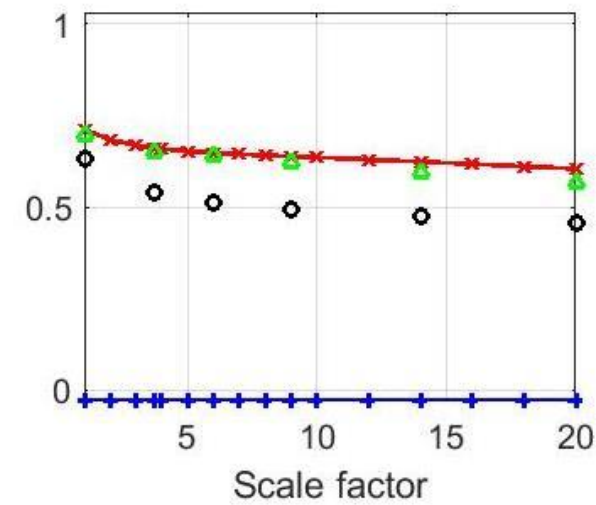
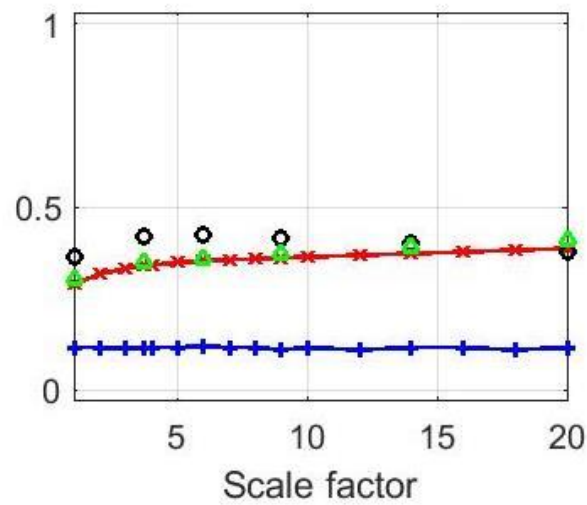
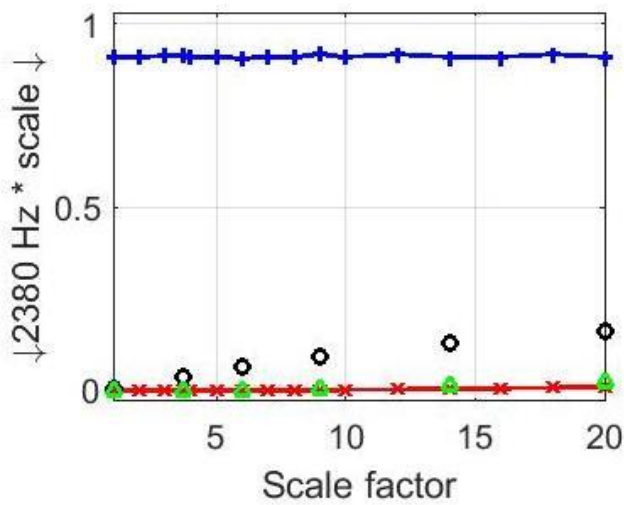
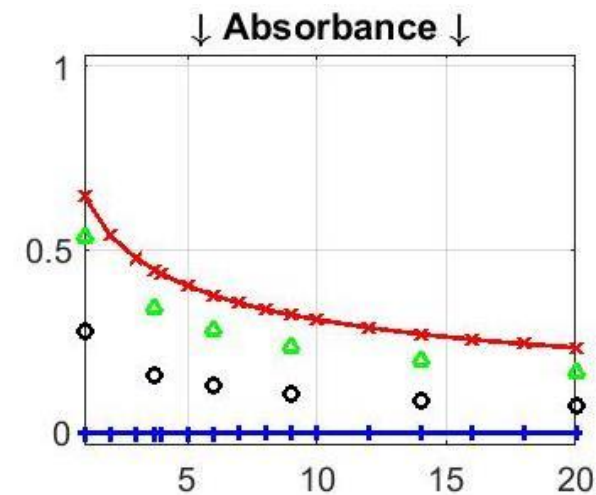
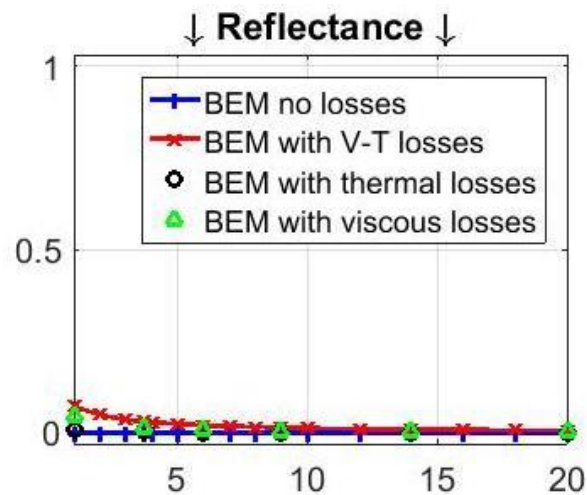
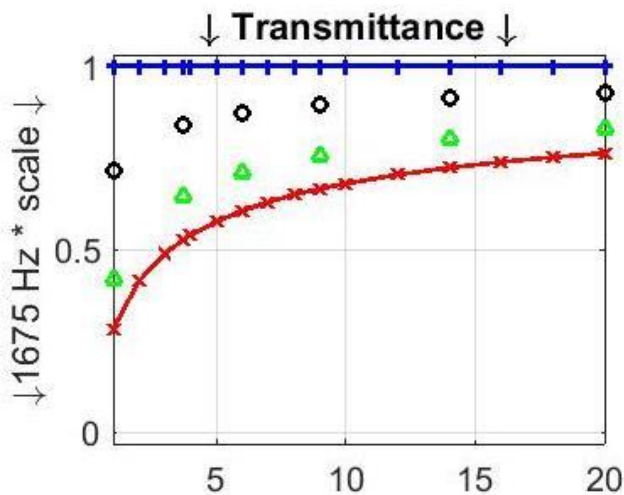


f (Hz)	viscous layer (μm)	thermal layer (μm)
100	210	250
1000	66	79
10000	21	25
20000	15	16

Double-negative metamaterial



Double-negative metamaterial



METAgenierie2017, 2-7 July

Visco-thermal effects:

- Visco-thermal losses **should be considered** in order to obtain a realistic design of single- and double-negative metamaterials.
- The double-negative phenomena might be **suppressed by losses**.
- High loss is **persistent** at the double-negative band, even when the structure is **scaled up**.
- Double-negative metamaterials might be a **good alternative to conventional absorbers** for specific situations, e.g., when dealing low frequencies or when the excitation is narrow banded.
- Some properties of metamaterials may survive losses, with the proper design:
 - Use less rows of units.
 - Find resonators with less losses (e.g. with optimization)

Recent Results on Acoustic metamaterials

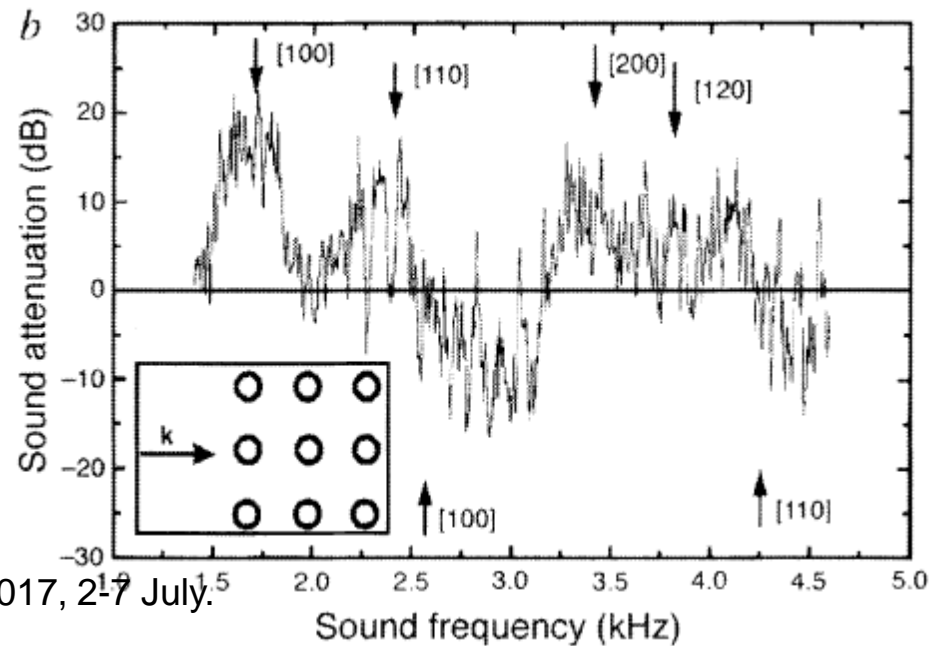
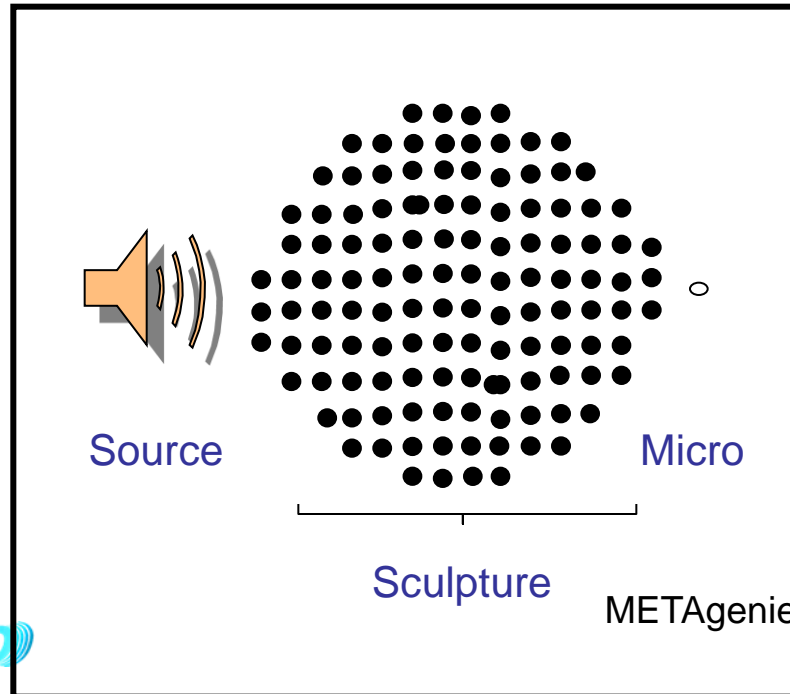
OUTLINE

1. Introduction
2. Acoustic metamaterials with negative parameters
3. Viscothermal effects in acoustic metamaterials with double-negative parameters
4. **Sound absorption and redirection with sonic crystals based on metamaterial units**

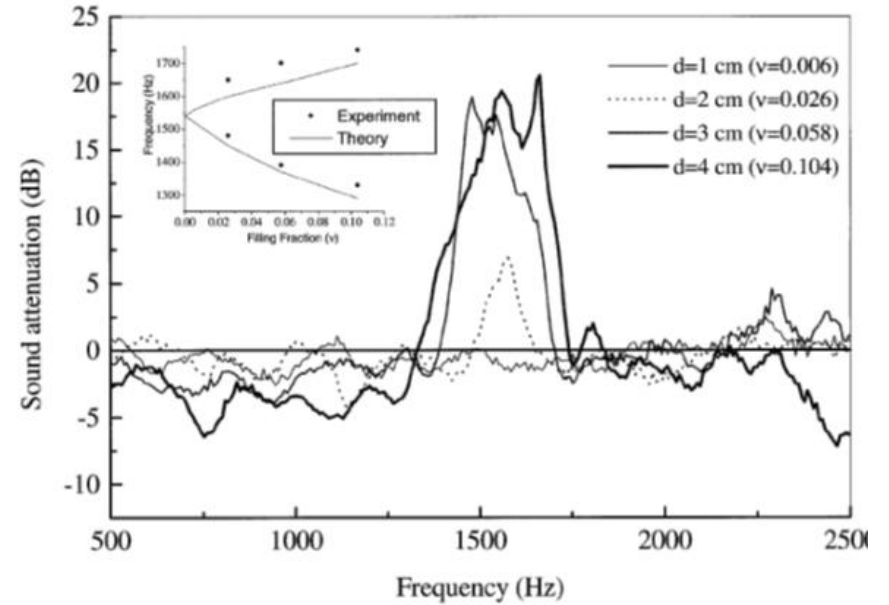
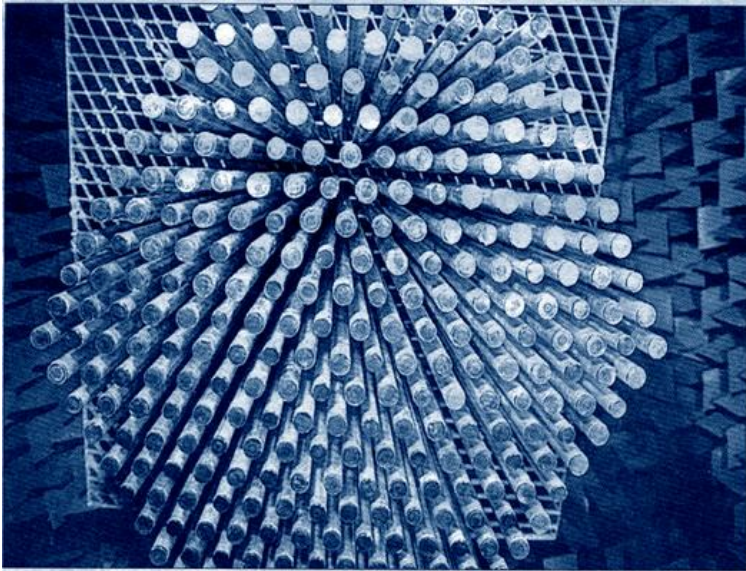
Sonic crystals / Phononic Crystals

Eusebio Sempere (Spanish artist)

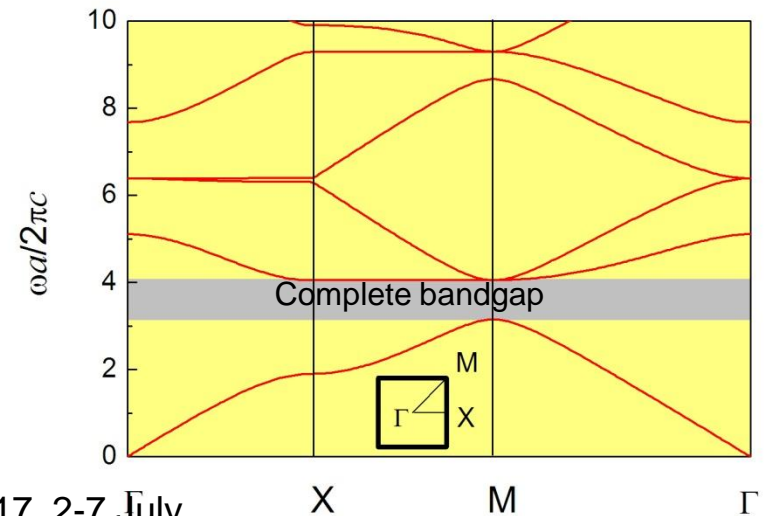
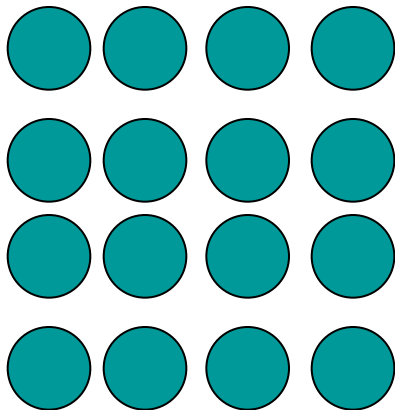
R. Martinez-Sala *et al.* **Nature (1995)**



Transmission properties of sonic crystals



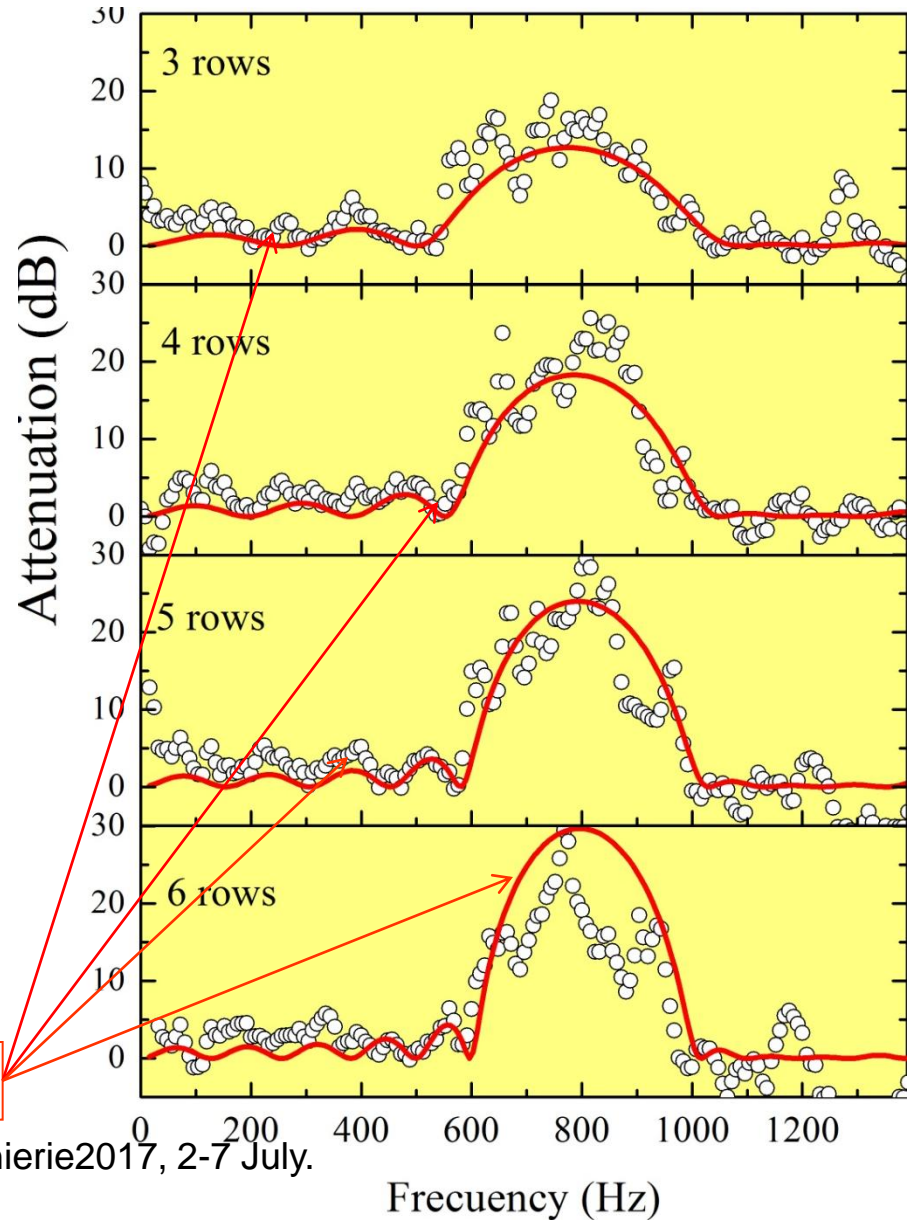
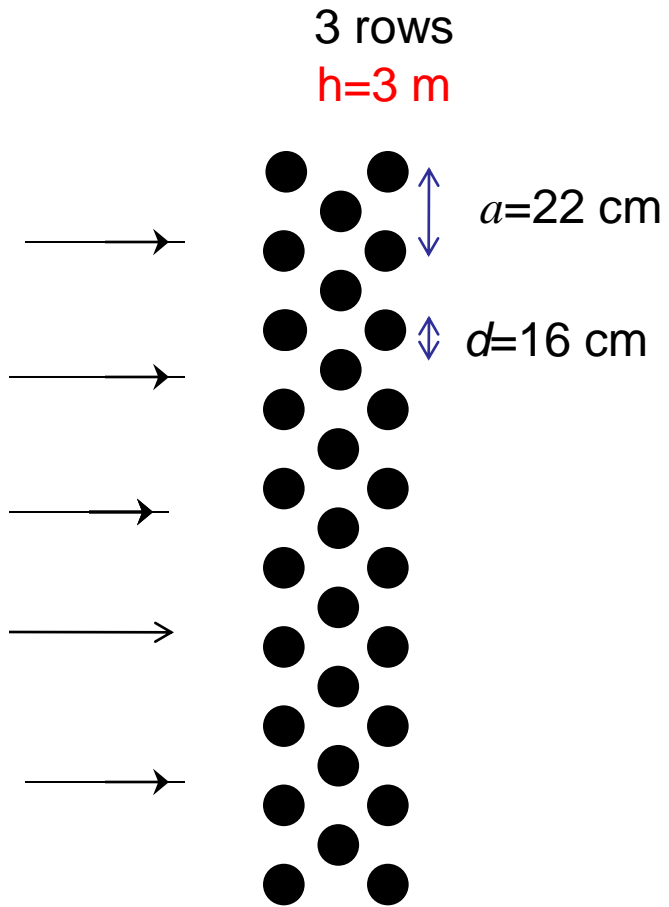
$f=0.4$



METAgénierie2017, 2-7 July.

Phys. Rev. Lett. **80**, 5325 (1998)

What is the minimum number of rows?



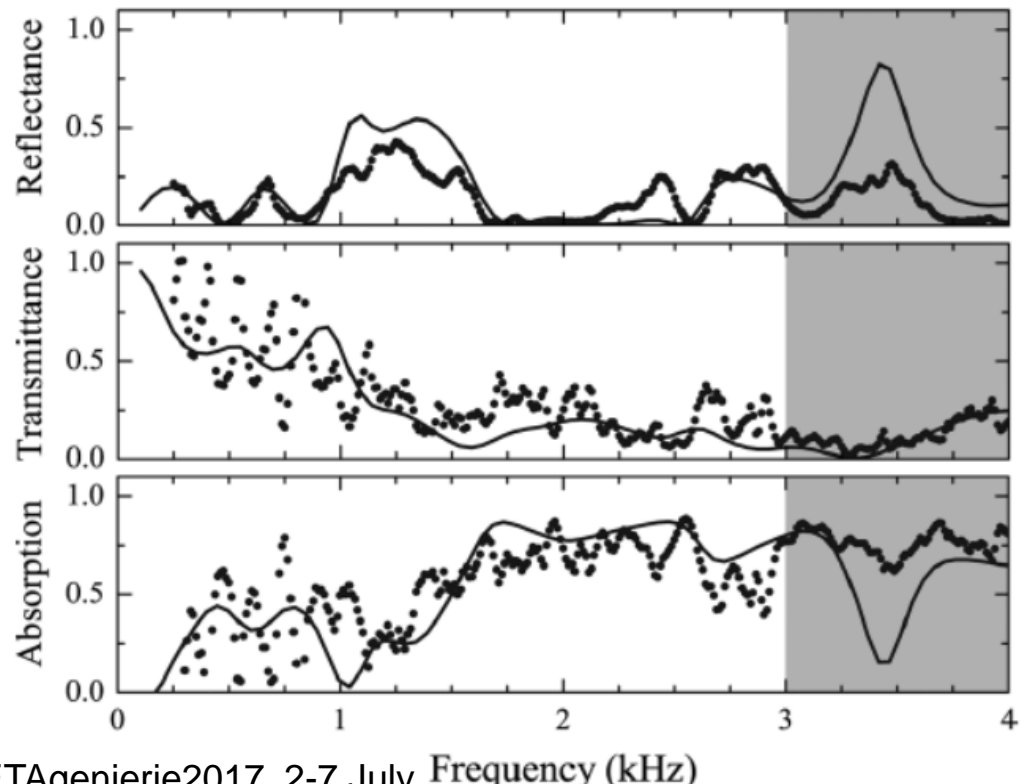
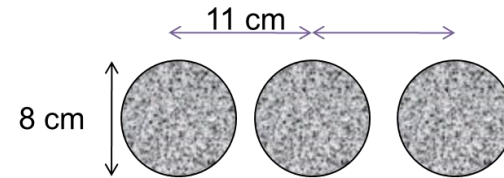
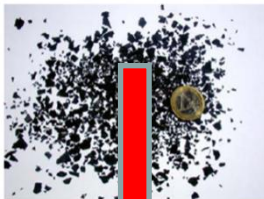
Multiple scattering simulations

Noise barriers made of porous materials (rubber crumb)

300 million used tires are removed annually in the 27 EU Member states

- Perforated shells with mm-size holes are (almost) acoustically transparent.
- They are used as containers of absorbing materials (rubber crumb, fiber glass, etc..).

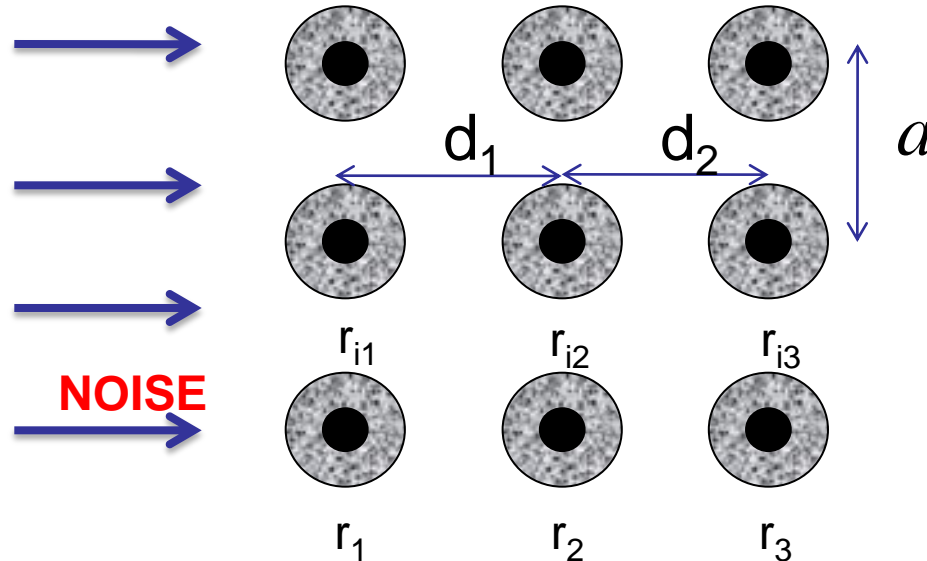
Rubber crumb: 0-7mm



METAgenierie2017, 2-7 July. Frequency (kHz)

Sanchez-Dehesa et al., JASA, 129, 1173 (2011).

Barriers for traffic noise: OPTIMIZATION APPROACH



Objective function: **index of isolation for airborne noise**

$$DL_R = -10 \log \left| \frac{\sum_{i=1}^{18} 10^{0.1L_i} 10^{-0.1R_i}}{\sum_{i=1}^{18} 10^{0.1L_i}} \right| \quad (\text{UNE-EN 1793})$$

L_i is the **normalized spectrum of traffic noise** (defined in 18 thirds of octave band between 100 Hz and 5kHz)

R_i is the **transmission loss by the barrier**

Class B₁: $DL_R < 15$ dB

Class B₂: $DL_R = 15$ dB to 24 dB

Class B₃: $DL_R > 24$ dB

Barriers for traffic noise based on rubber crumb

Table 1

Barrier parameters (see Fig. 2) obtained from the optimization algorithm. Length dimensions are in cm. Last row contains the airborne insulation index DL_R . Note that the highest quality barriers, class B_3 , according to the European normative is achieved when $DL_R > 24$ dB [16].

	T		T_{eff}		T'_{eff}		T''_{eff}	
	□	△	□	△	□	△	□	△
r_1	10.0	10.0	10.0	10.0	10.0	10.0	10.0	10.0
r_2	10.0	10.0	10.0	10.0	10.0	10.0	10.0	10.0
r_3	10.0	10.0	10.0	10.0	10.0	10.0	10.0	10.0
r_{i1}	4.6	10.0	3.4	5.1	4.2	7.3	4.5	9.2
r_{i2}	4.3	5.0	4.0	4.3	4.3	4.1	4.3	3.8
r_{i3}	4.7	9.5	4.5	10.0	4.6	10.0	4.7	9.4
d_1	32.1	18.2	31.2	18.2	31.8	18.2	32.1	18.2
d_2	48.9	18.2	49.8	18.2	49.1	18.2	48.9	18.2
D	40.0	21.0	40.0	21.0	40.0	21.0	40.00	21.0
DL_R (dB)	7.2	18.6	6.7	16.6	14.0	24.7	21.1	32.1

Class B_3 : $DL_R > 24$ dB

Noise barriers based on μ -perforated shells

Properties of flat perforated panels

- Impedance of a flat perforated panel (Ingard, Allard, Atalla, Åbom, etc.):

$$Z_p = \frac{i\omega\rho_0 t}{\sigma} \left[1 - \frac{2}{s\sqrt{-i}} \frac{J_1(s\sqrt{-i})}{J_1(s\sqrt{-i})} \right]^{-1} + \frac{4}{\sigma} \sqrt{2\eta_0\omega\rho_0} + \frac{i\omega\rho_0}{\sigma} \frac{16r}{3\pi} \left(1 - 2.5\sqrt{\frac{\sigma}{\pi}} \right)$$

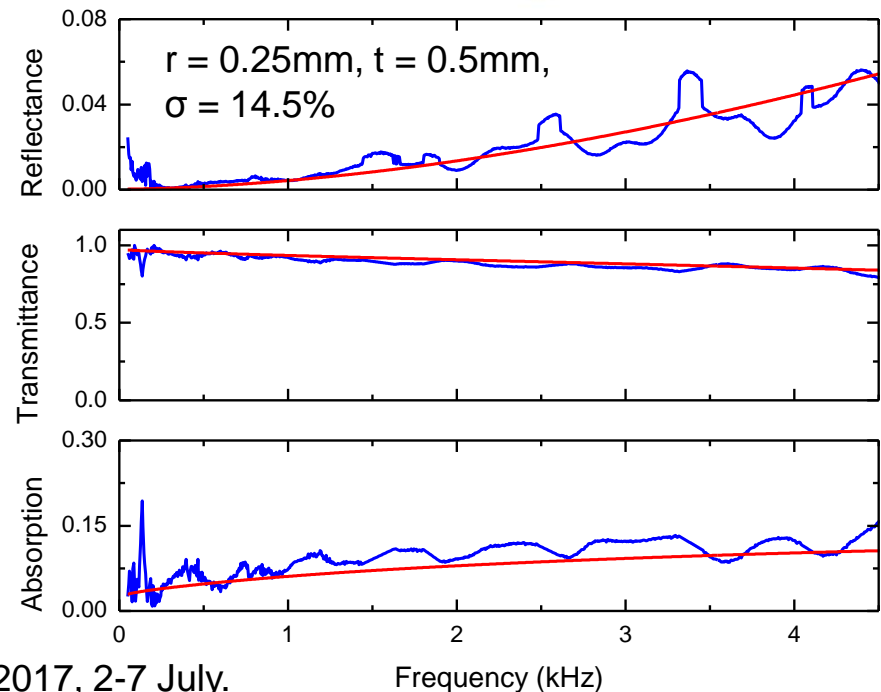


For large holes $r \gg \delta = \sqrt{\frac{2\eta_0}{\rho_0\omega}}$

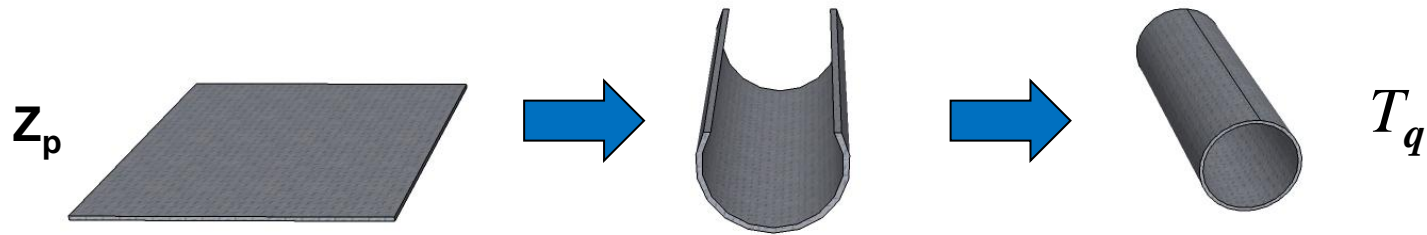
and moderate filling fractions σ ,
the panel has low Z_p .

Small holes ($r \approx 1 \mu\text{m}$) lead to
absorbing panels.

D.-Y. Maa, JASA 104, 2861 (1998).



Perforated cylindrical shells multiple scattering approach



- The T-matrix of a perforated shell is obtained from an impedance based model:

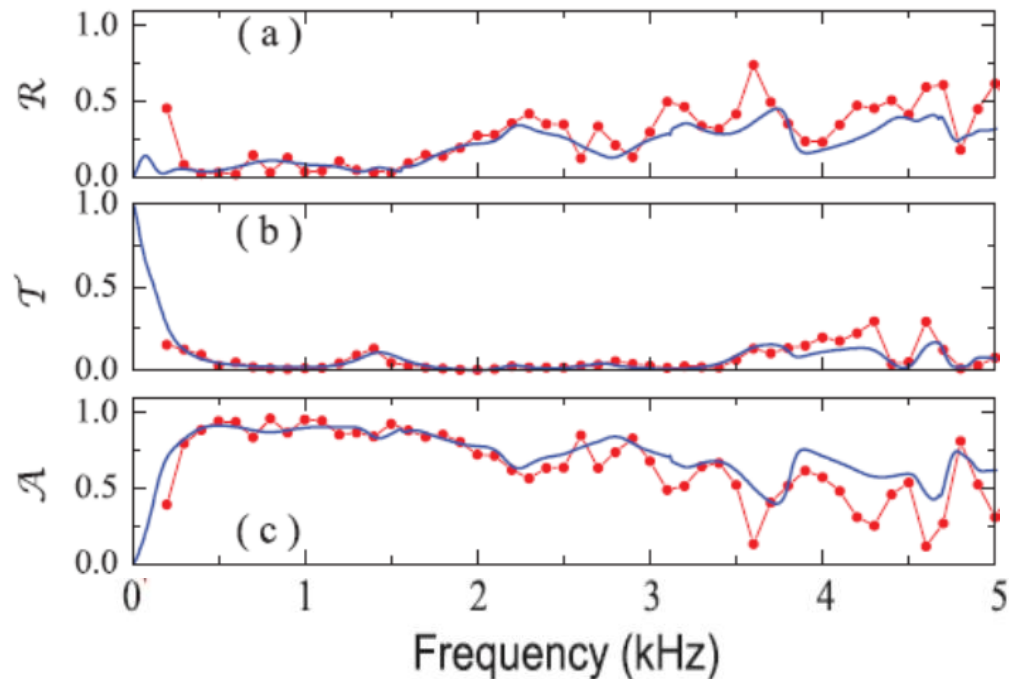
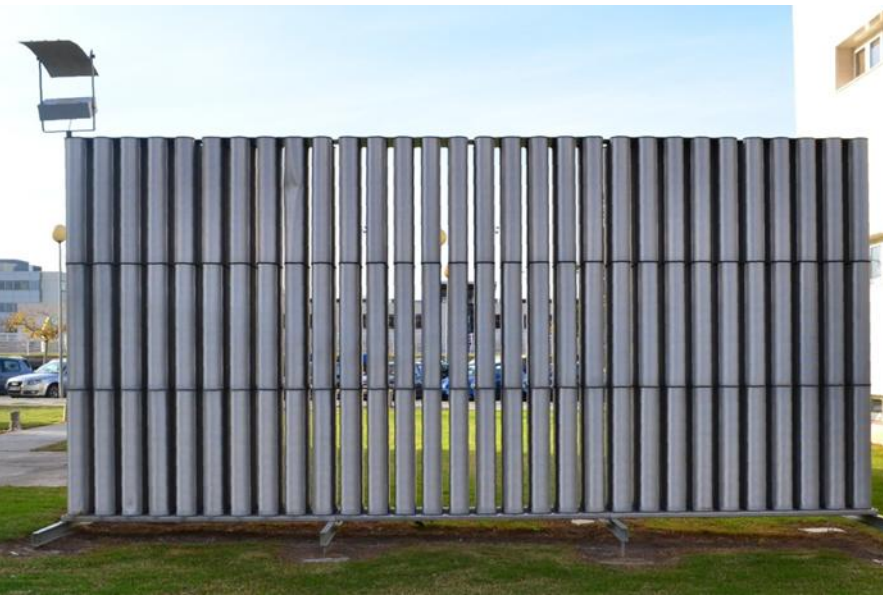
$$T_q = - \frac{\rho_q \begin{pmatrix} J'_q(\kappa_0 R^+) \\ H'_q(\kappa_0 R^+) \end{pmatrix} - \begin{pmatrix} J_q(\kappa_0 R^+) \\ H_q(\kappa_0 R^+) \end{pmatrix}}{\begin{pmatrix} J_q(\kappa_0 R^-) \\ J'_q(\kappa_0 R^-) \end{pmatrix} - \frac{iZ_p k_0}{\omega \rho_0} \begin{pmatrix} J_q(\kappa_0 R^-) \\ J'_q(\kappa_0 R^-) \end{pmatrix}} \rho_q = \frac{\begin{pmatrix} J_q(\kappa_0 R^-) \\ J'_q(\kappa_0 R^-) \end{pmatrix} - \frac{iZ_p k_0}{\omega \rho_0} \begin{pmatrix} J_q(\kappa_0 R^-) \\ J'_q(\kappa_0 R^-) \end{pmatrix}}{\begin{pmatrix} J_q(\kappa_0 R^-) \\ J'_q(\kappa_0 R^-) \end{pmatrix}}$$

- Transmission through a lattice of perforated shells has been calculated using Multiple Scattering Theory

Attenuation of broadband noise: SC made of μ -perforated shells

- μ -perforated shells are interesting due to the absorptive properties of μ -perforations.

3 rows of 30 cylinders ($R=16\text{cm}$, $h=3\text{m}$) and $a=22\text{cm}$.



Acoustic barriers based on lattices of μ -perforated shells



PROS:

- No foundations are needed
- The flow of wind passes through the barrier
- Lightweight and robust
- Great aesthetic



CONS:

- Expensive
(The cost can be substantially reduced by using massive manufacturing methods)



METAgenierie2017, 2-7 July.

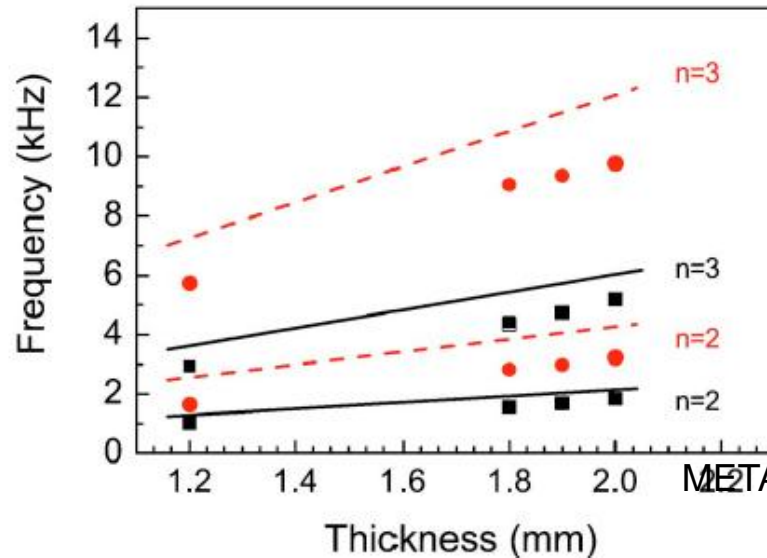
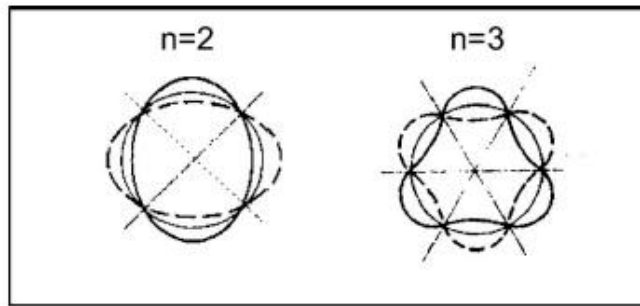
OUTLINE

Redirection of sound with a sonic crystal made of perforated thin shells

Fano-like resonance phenomena by flexural shell modes in sound transmission through two-dimensional periodic arrays of thin-walled hollow cylinders

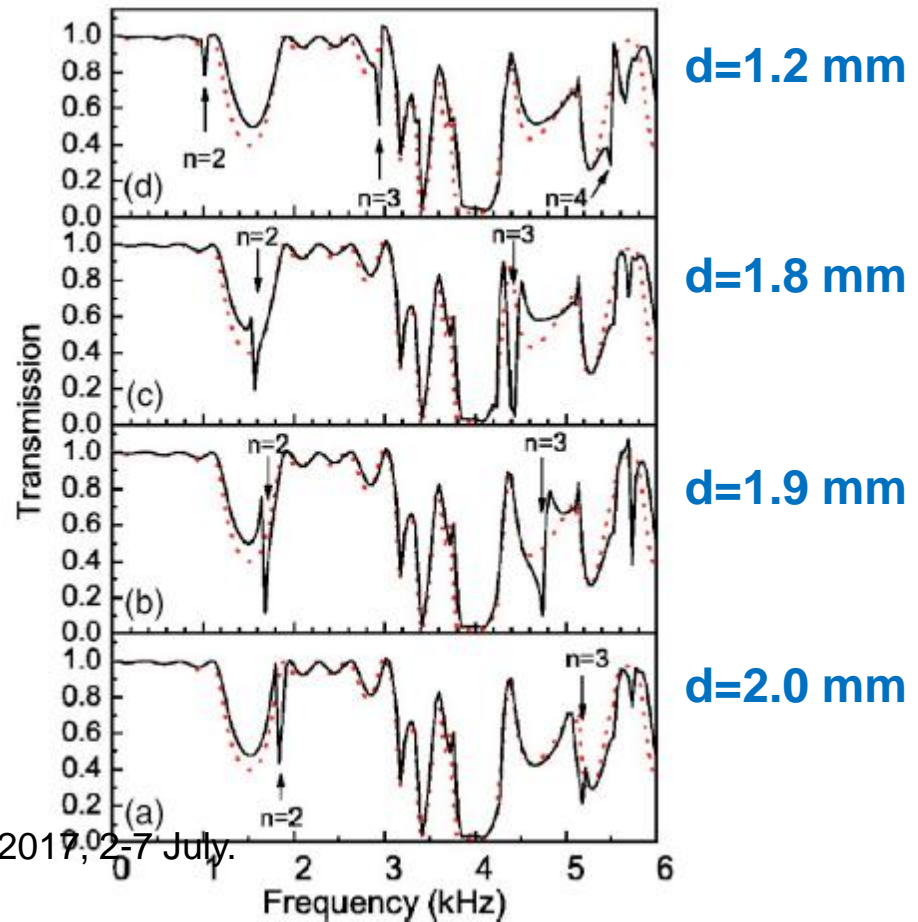
Yuriy A. Kosevich,^{1,*} Cecile Goffaux,^{2,†} and Jose Sánchez-Dehesa^{1,‡}

$$\nu_n = \frac{n(n^2 - 1)}{\sqrt{1 + n^2}} \frac{d}{r^2} \frac{C_{ts}}{4\pi}$$



4 layers Sonic Cristal
 $a=11$ cm

Thickness

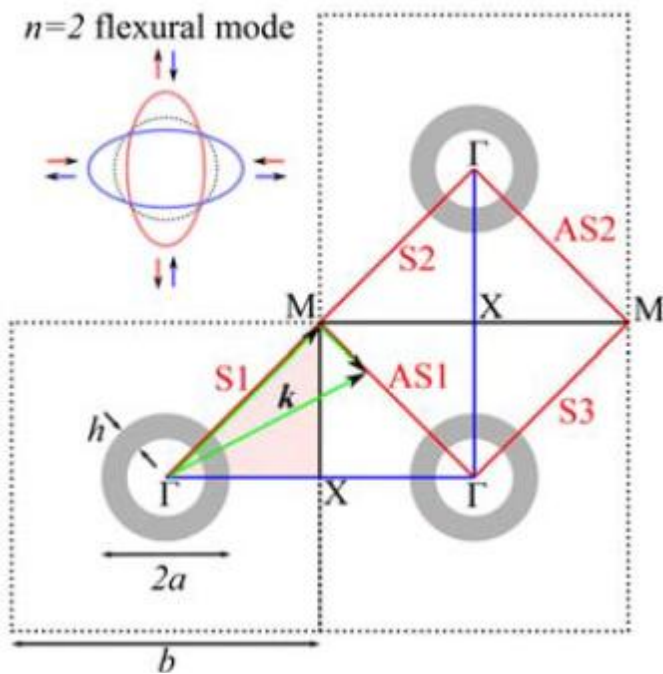


Acoustic Poisson-like Effect in Periodic Structures

Alexey S. Titovich¹, Andrew N. Norris¹

¹ Mechanical and Aerospace Engineering, Rutgers University, 98 Brett Road, Piscataway, NJ, USA,
alexey.titovich@rutgers.edu, norris@rutgers.edu

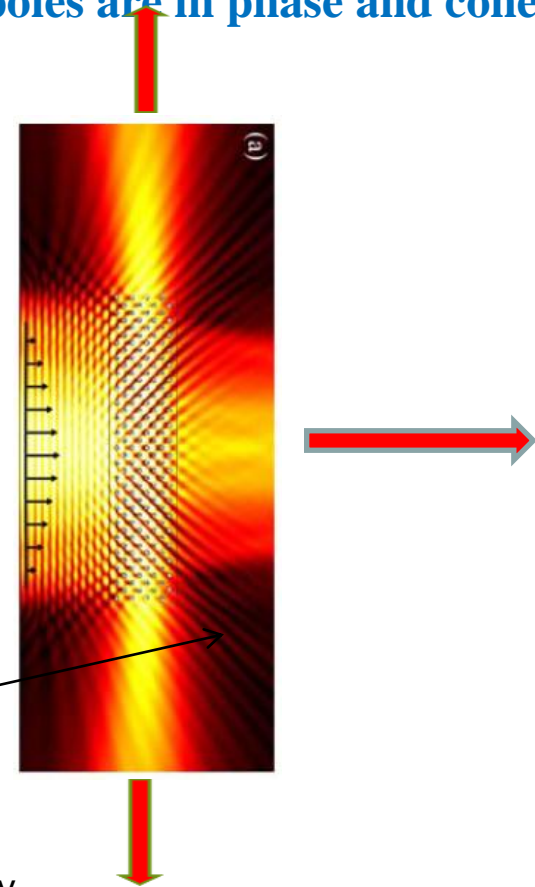
if λ is on the order of the spacing, the scattered quadrupoles are in phase and coherently redirect acoustic energy by 90 degrees.



Gaussian beam

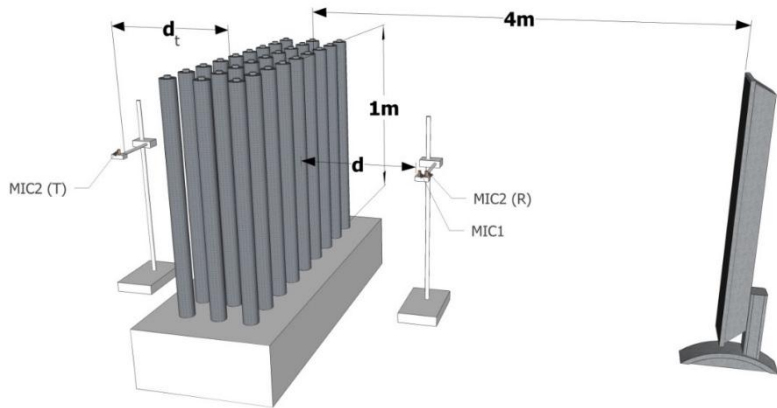
**Sonic Cristal
(8 layers)**

METAgenierie2017, 2-7 July.

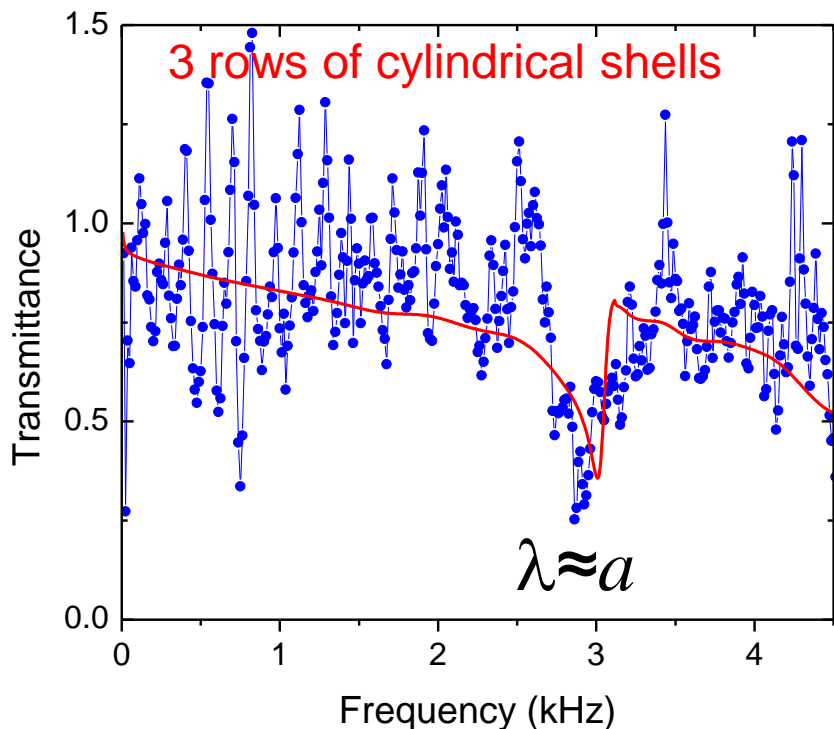


JASA **139**, 3353 (2016)

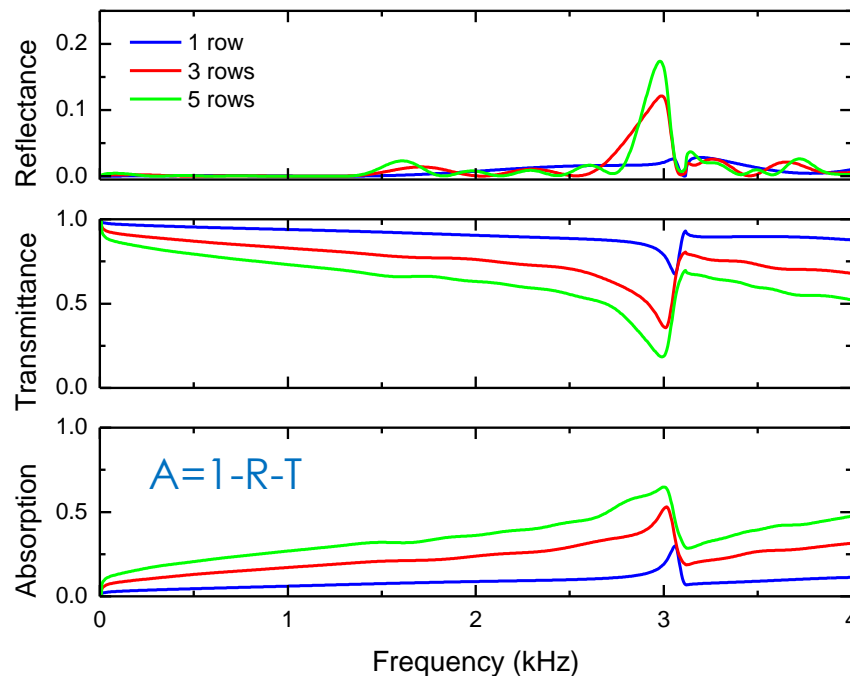
Sound redirection by Wood anomalies



$R = 4\text{cm}$
 $r = 0.25\text{mm}$
 $t = 0.50\text{mm}$
 $\sigma = 14.5\%$
 $a = 11\text{cm}$



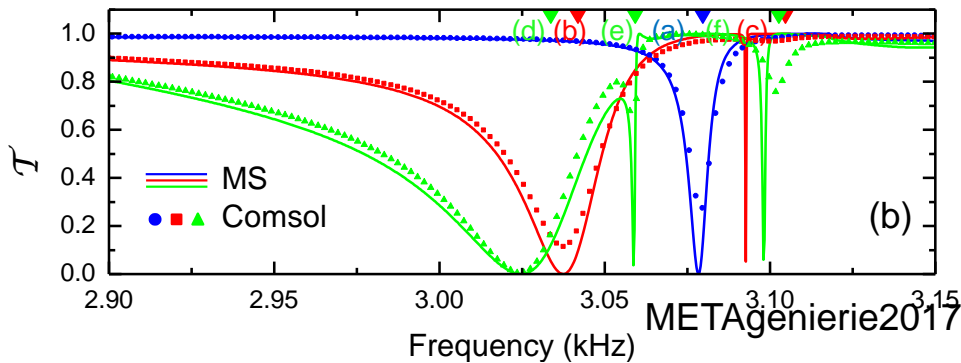
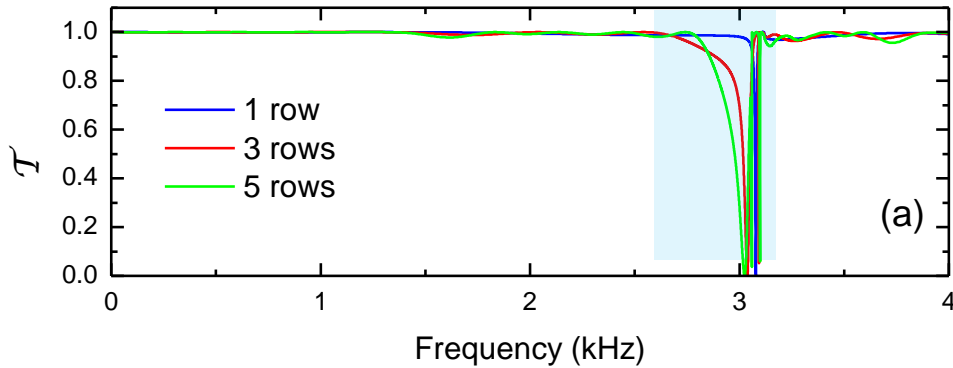
Numerical simulations ($\eta_0 \neq 0$)



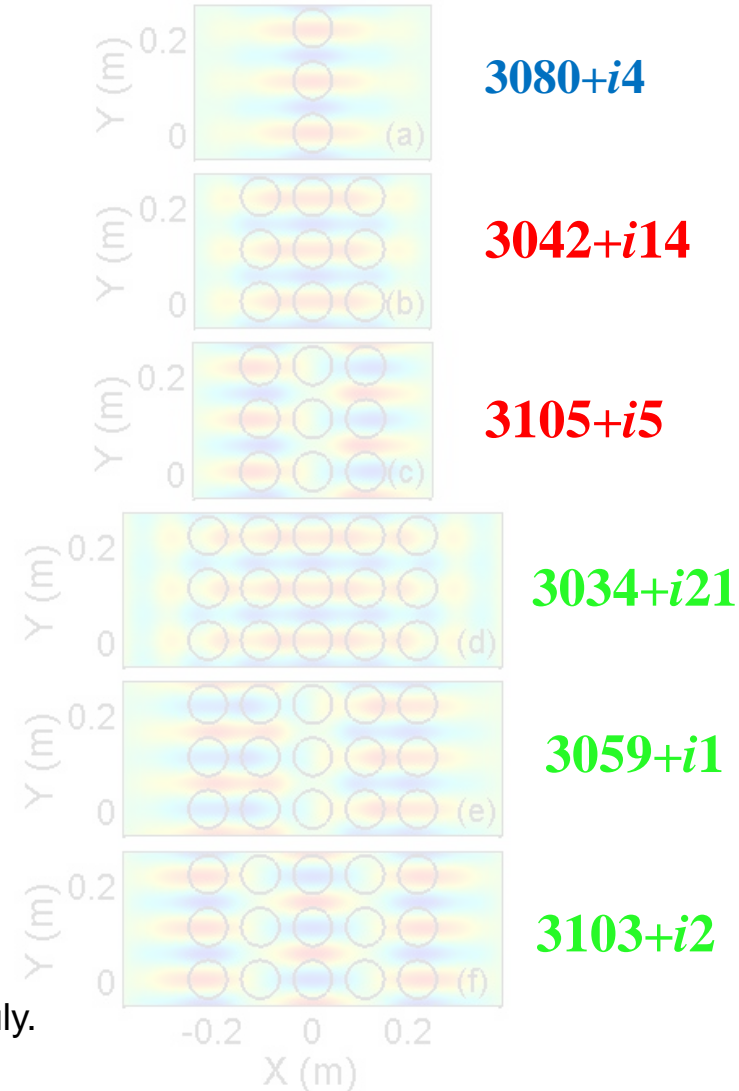
- Absorption enhancement occurs at the frequencies with minimum transmittance.

Non-dissipative case ($\eta_0=0$)

- Full transmission occurs except at around 3kHz.
- Total reflection is found at $\lambda \approx a$ even for one row.
- **T minima show Fano-like profiles indicating the excitation of resonant Wood anomalies.**



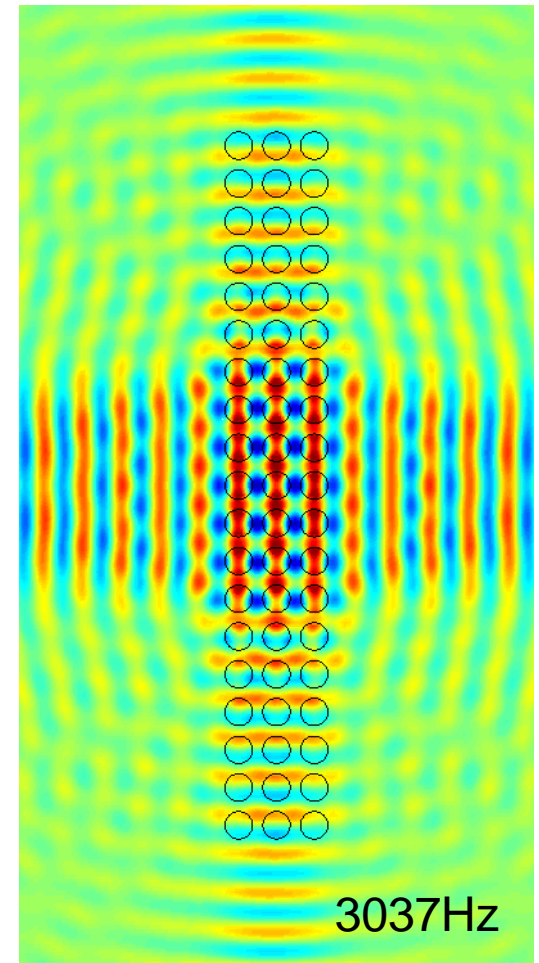
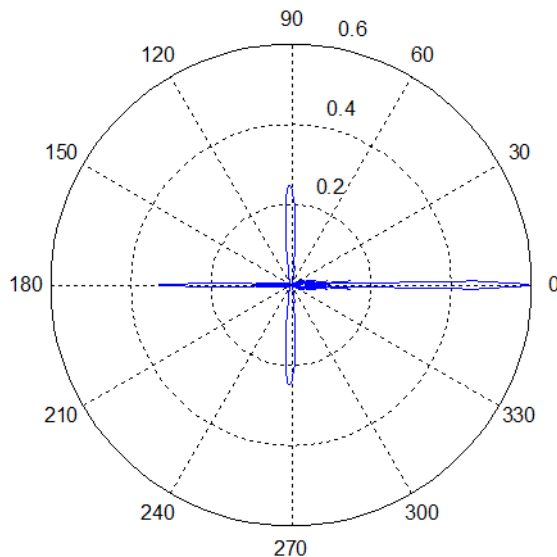
Frequency



Energy redirection due to Wood anomalies

- The resonant anomaly involves modes guided along the slab.
- Propagating modes are observed when exciting the slab with a Gaussian beam.

Pressure at the far field (a. u.)

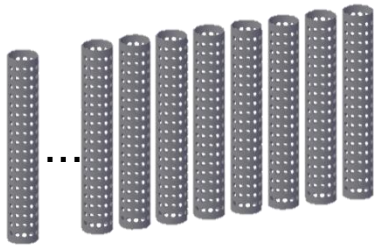


METAgenierie2017, 2-7 July.

García-Chocano & JSD, APL 106, 124104 (2015)

Energy splitting with a linear chain of perforated thin shells

The case of a linear chain



Incident plane wave:

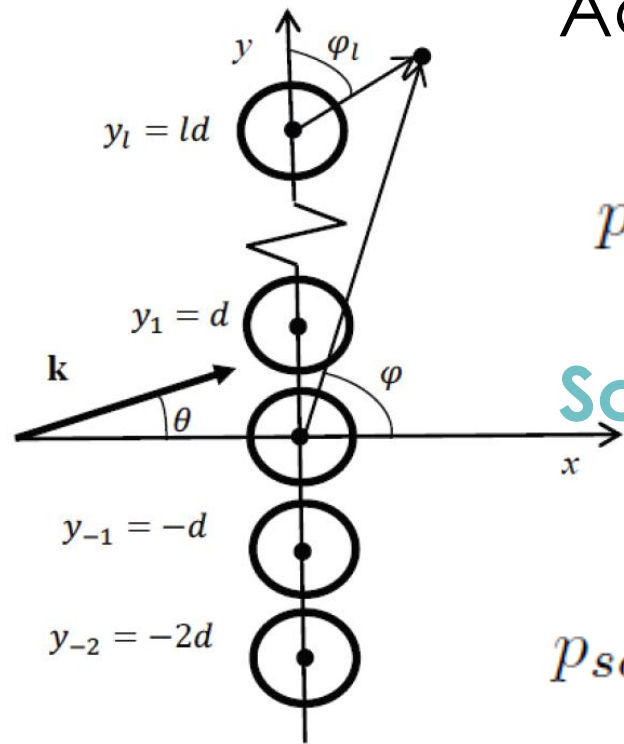
$$p(\mathbf{r}) = p_0 \exp(i\mathbf{k} \cdot \mathbf{r})$$

Acoustic field **inside each shell**:

$$p_{in}(r_l, \varphi_l) = \sum_{n=-\infty}^{\infty} C_{ln} J_n(kr_l) e^{in\varphi_l}$$

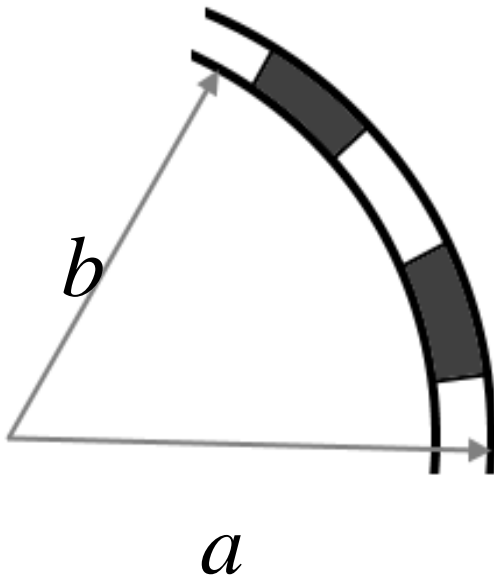
Scattered acoustic field:

$$p_{sc}(r, \varphi) = \sum_{l'} \sum_{n=-\infty}^{+\infty} B_{l'n} H_n(kr_{l'}) e^{in\varphi_{l'}}$$



Boundary conditions

The **impedance approach** is used to match the acoustic fields *inside* and *outside* each individual microperforated shell



continuity of normal velocity

$$v_r|_{r=a} = v_r|_{r=b} = \frac{p|_{r=b} - p|_{r=a}}{Z_p}$$

normal velocity is due to the discontinuous jump of pressure

Effective acoustic impedance of the flat plate:

$$Z_p = -\frac{i\omega\rho_0}{\sigma} \left[h + \frac{16s}{3\pi} \left(1 - 2.5 \sqrt{\frac{\sigma}{\pi}} \right) \right]$$

Dah-You Maa, J. Acoust. Soc. Am. **104**, 2861 (1998).

Acoustic band structure: $\omega(q)$

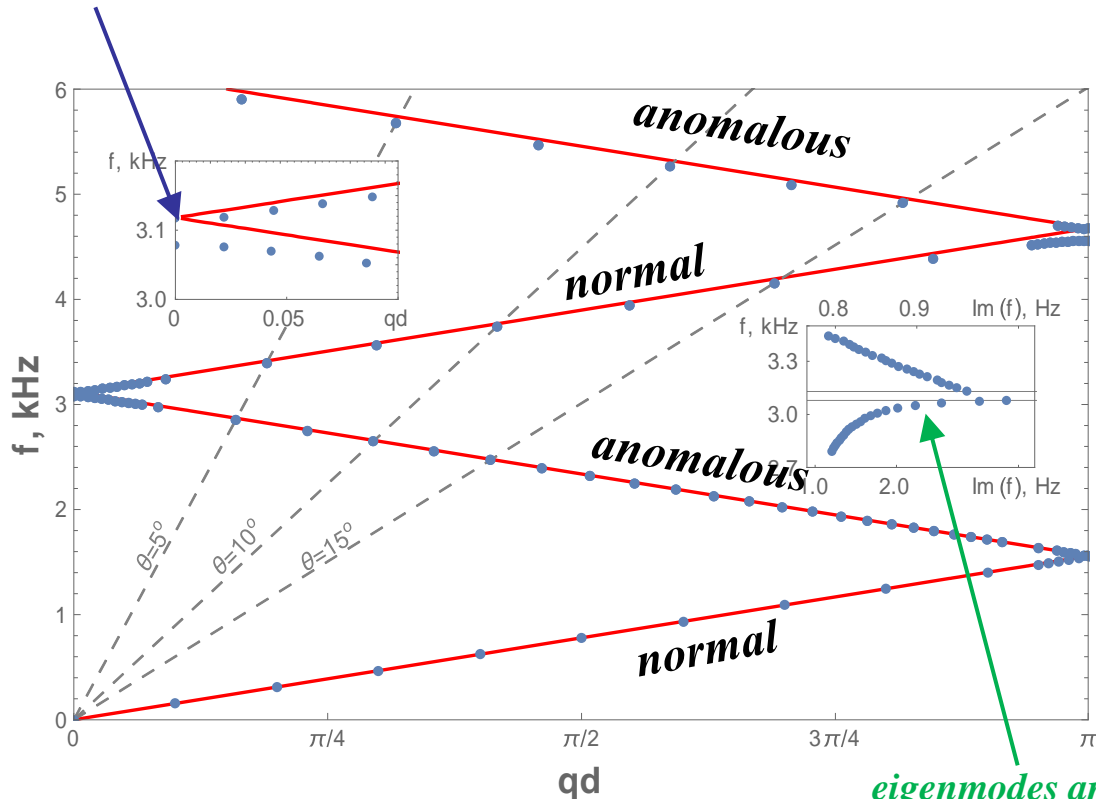
After some algebra...

$$\det |\mathcal{S}_n \delta_{nn'} + F(n' - n)| = 0.$$



$$n = 0, \pm 1, \pm 2, \dots$$

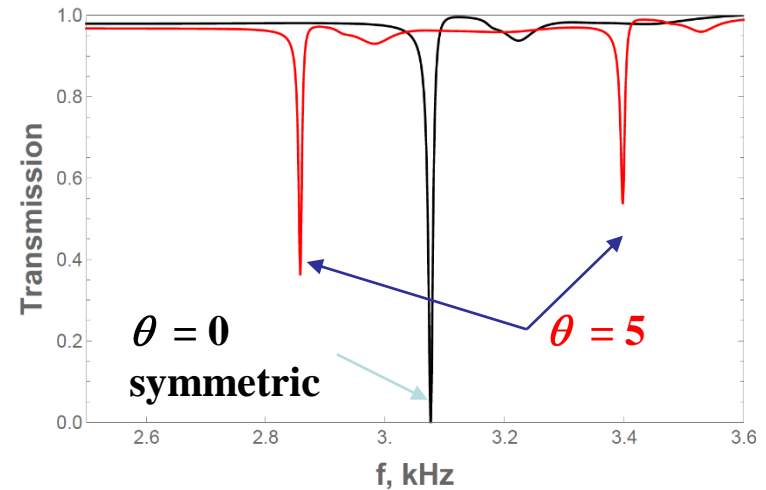
asymmetric bandgap



The eigenmode is excited

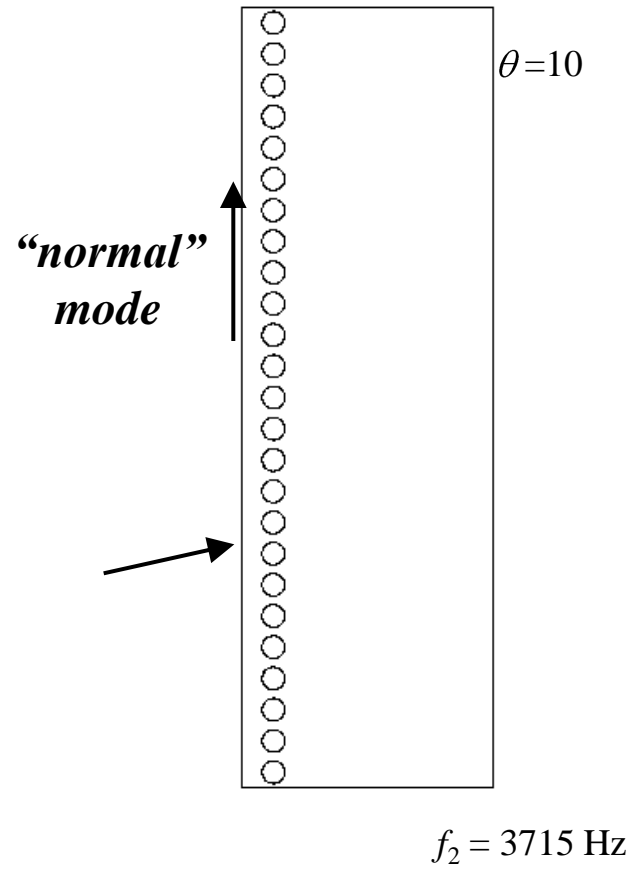
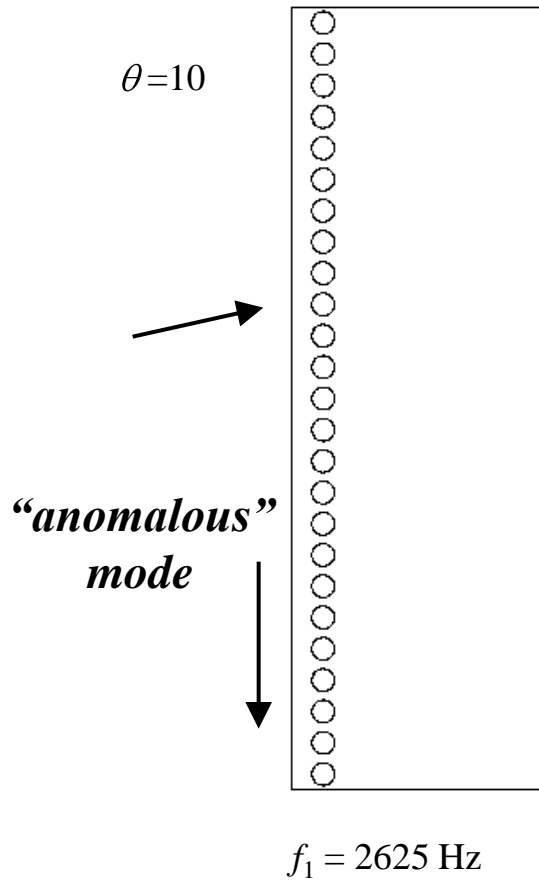
$$k_y = (2\pi f/c) \sin \theta = q(f)$$

infinite chain



*eigenmodes are leaky
(even w/o viscosity),
so they can be excited*

Eigenmode excitation

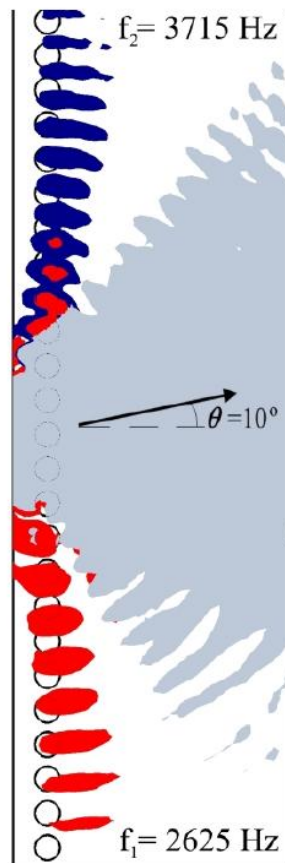


Splitting of a bi-frequency signal

25 perforated shells

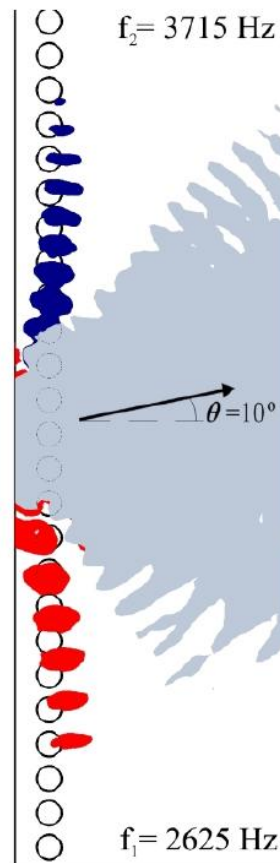
inviscid air

8% (low f. component)
10% (high f. component)



viscous air

5% (low f. component)
7% (high f. component)



Mixture of the two
sound waves

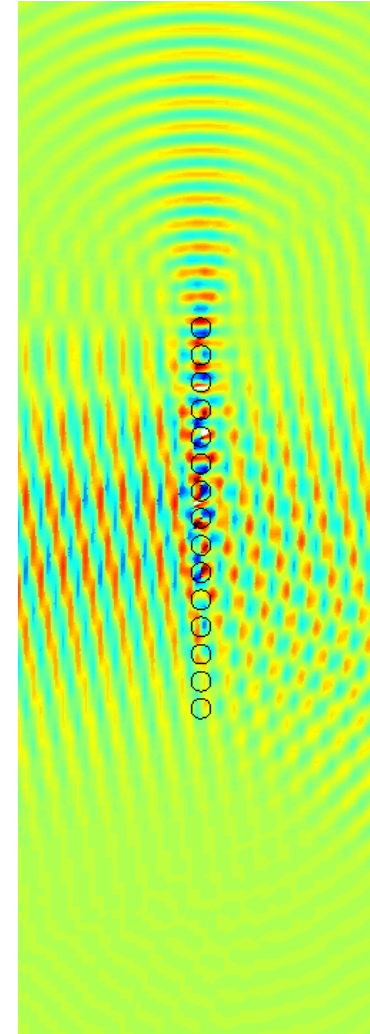
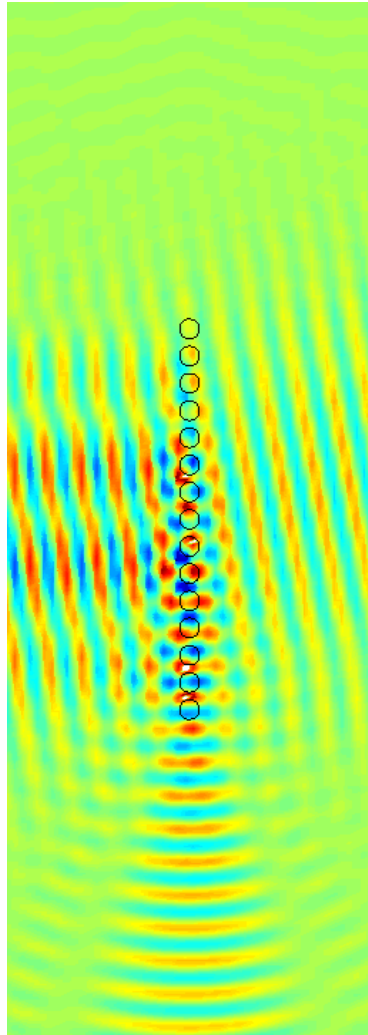
Low frequency component (in red) propagates against the *natural* direction!!

METAgenierie2017, 2-7 July.

Bozhko, **JSD**, Cervera and Krokhin, Phys. Rev. Appl. (in press)

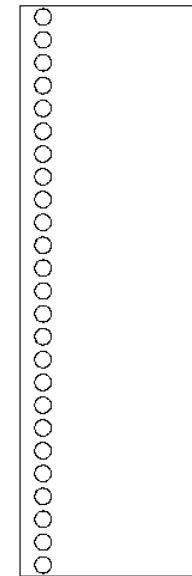
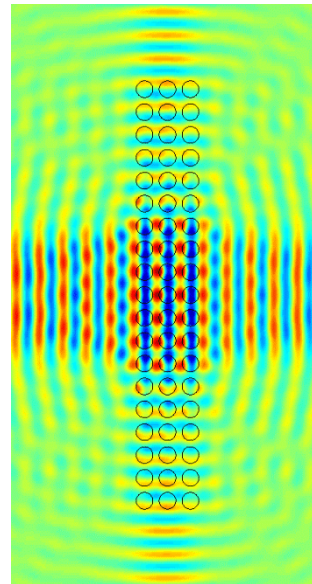
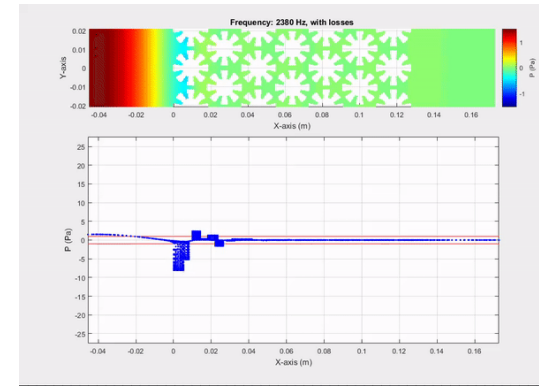
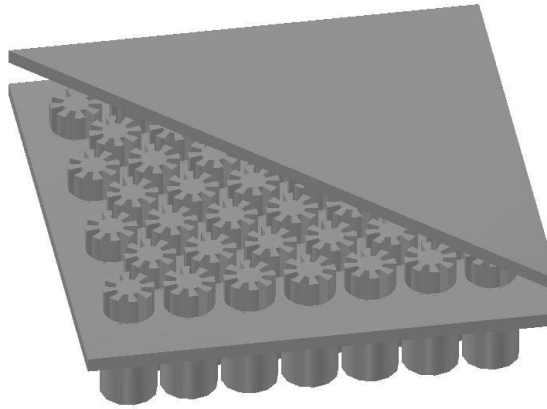
Splitting of a bi-frequency signal

Numerical experiments (FEM simulations)



$f_1 = 2520$ Hz METAgenierie2017, 2-7 July. $f_1 = 3520$ Hz

Summary



Thanks for your attention!

METAgenierie2017, 2-7 July